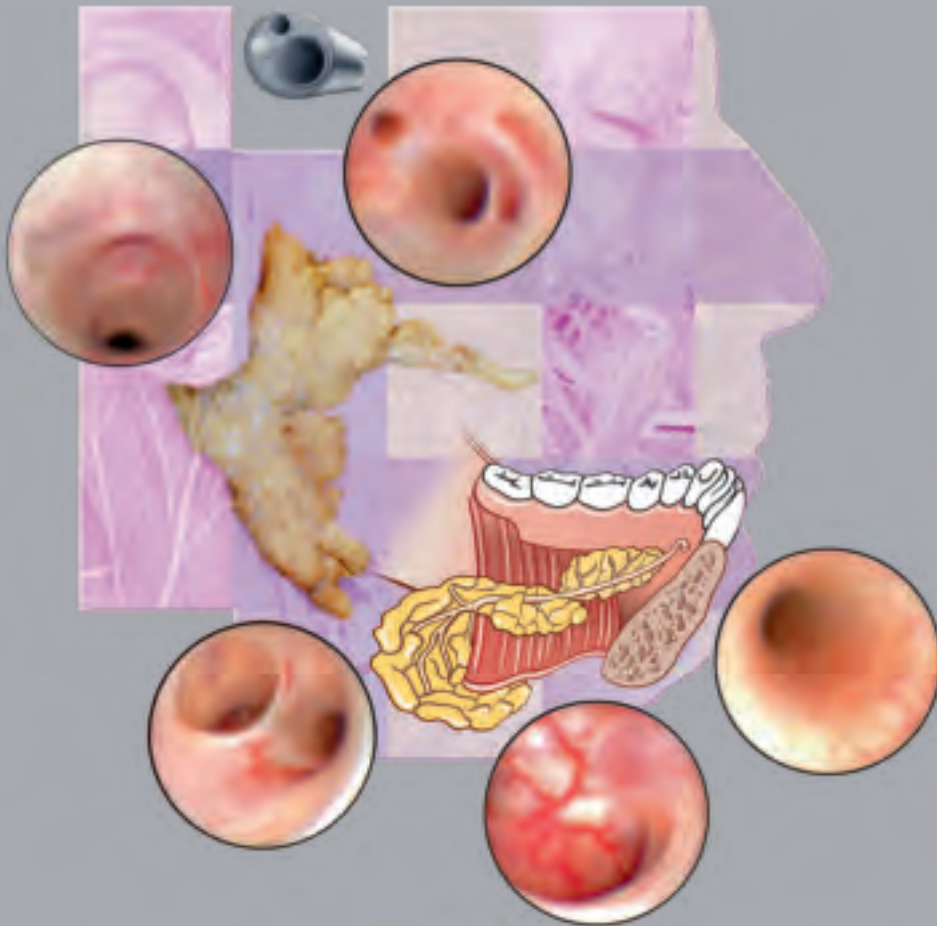


THE ERLANGEN SALIVARY GLAND PROJECT

Part I: Sialendoscopy in Obstructive Diseases
of the Major Salivary Glands



Heinrich IRO, Johannes ZENK
Michael KOCH, Alessandro BOZZATO



The Wolf and the Crane – A Fable of Aesop

A Wolf was feasting greedily on a sheep he had killed, when suddenly a bone became stuck in his throat. He offered a handsome reward to anyone who could relieve his suffering. The Crane agreed to try. Fortunately, she was able to extract the bone with her beak, and she asked for her reward.

“What!” snarled the Wolf. “Isn’t it enough that you have put your head inside a Wolf’s mouth and taken it out again safely? Go home, and be grateful that you’re still alive!”

In serving the wicked, expect no reward,
and be thankful if you escape injury for your pains.

Endo:Press®

THE ERLANGEN SALIVARY GLAND PROJECT

Part I: Sialendoscopy in Obstructive Diseases
of the Major Salivary Glands

Prof. Heinrich IRO, M.D.
Prof. Johannes ZENK, M.D.
Michael KOCH, M.D.
Alessandro BOZZATO, M.D.

Erlangen University Medical School
Dept. of Otorhinolaryngology, Head and Neck Surgery
Salivary Gland Center – Erlangen, Germany

Illustrations:

Katja Dalkowski, M.D., Grasweg 42,
D-91054 Buckenhof, Germany
E-mail: kdalkowski@online.de

Important notes:

Medical knowledge is ever changing. As new research and clinical experience broaden our knowledge, changes in treatment and therapy may be required. The authors and editors of the material herein have consulted sources believed to be reliable in their efforts to provide information that is complete and in accord with the standards accepted at the time of publication. However, in view of the possibility of human error by the authors, editors, or publisher, or changes in medical knowledge, neither the authors, editors, publisher, nor any other party who has been involved in the preparation of this booklet, warrants that the information contained herein is in every respect accurate or complete, and they are not responsible for any errors or omissions or for the results obtained from use of such information. The information contained within this booklet is intended for use by doctors and other health care professionals. This material is not intended for use as a basis for treatment decisions, and is not a substitute for professional consultation and/or use of peer-reviewed medical literature.

Some of the product names, patents, and registered designs referred to in this booklet are in fact registered trademarks or proprietary names even though specific reference to this fact is not always made in the text. Therefore, the appearance of a name without designation as proprietary is not to be construed as a representation by the publisher that it is in the public domain.

The use of this booklet as well as any implementation of the information contained within explicitly takes place at the reader's own risk. No liability shall be accepted and no guarantee is given for the work neither from the publisher or the editor nor from the author or any other party who has been involved in the preparation of this work. This particularly applies to the content, the timeliness, the correctness, the completeness as well as to the quality. Printing errors and omissions cannot be completely excluded. The publisher as well as the author or other copyright holders of this work disclaim any liability, particularly for any damages arising out of or associated with the use of the medical procedures mentioned within this booklet.

Any legal claims or claims for damages are excluded.

In case any references are made in this booklet to any 3rd party publication(s) or links to any 3rd party websites are mentioned, it is made clear that neither the publisher nor the author or other copyright holders of this booklet endorse in any way the content of said publication(s) and/or web sites referred to or linked from this booklet and do not assume any form of liability for any factual inaccuracies or breaches of law which may occur therein. Thus, no liability shall be accepted for content within the 3rd party publication(s) or 3rd party websites and no guarantee is given for any other work or any other websites at all.

The Erlangen Salivary Gland Project – Part I: Sialendoscopy in Obstructive Diseases of the Major Salivary Glands

Prof. **Heinrich Iro**, M.D.

Prof. **Johannes Zenk**, M.D.

Michael Koch, M.D.

Alessandro Bozzato, M.D.

Erlangen University Medical School

Dept. of Otorhinolaryngology, Head and Neck Surgery
Salivary Gland Center – Erlangen, Germany

Correspondence address of the author:

Universitätsklinikum Erlangen

Hals-Nasen-Ohren-Klinik, Kopf- und Halschirurgie

Direktor: Prof. Dr. Dr. h. c. **Heinrich Iro**

Waldstraße 1, 91054 Erlangen, Germany

<http://www.hno-klinik.uk-erlangen.de>

E-mail: hno@hno.imed.uni-erlangen.de

All rights reserved.

1st edition 2007

© 2015 **Endo:Press**® GmbH

P.O. Box, 78503 Tuttlingen, Germany

Phone: +49 (0) 74 61/1 45 90

Fax: +49 (0) 74 61/708-529

E-mail: endopress@t-online.de

No part of this publication may be translated, reprinted or reproduced, transmitted in any form or by any means, electronic or mechanical, now known or hereafter invented, including photocopying and recording, or utilized in any information storage or retrieval system without the prior written permission of the copyright holder.

Editions in languages other than English and German are in preparation. For up-to-date information, please contact **Endo:Press**® GmbH at the address shown above.

Design and Composing:

Endo:Press® GmbH, Germany

Printing and Binding:

Straub Druck + Medien AG

Max-Planck-Straße 17, 78713 Schramberg, Germany

07.15-0.7

ISBN 978-3-89756-149-6

Table of Contents

Preface

1.0	Anatomy of the Major Salivary Glands.....	6
2.0	Diagnostic Imaging.....	8
3.0	Sialendoscopy	11
3.1	Prerequisites for Endoscopic Examination of the Major Salivary Ducts.....	11
3.2	Instruments and Endoscopes.....	12
3.3	The Erlangen Endoscopy Set.....	13
3.4	Technique of Salivary Duct Endoscopy	17
3.5	Normal Findings in Sialendoscopy.....	20
4.0	Diagnostic and Interventional Sialendoscopy in Various Diseases	24
4.1	Sialolithiasis.....	24
4.2	Sialendoscopic Techniques in Noncalcified Obstructions.....	32
4.3	Follow-up Care	39
4.4	Morbidity and Complications.....	39
4.5	Indications and Contraindications to Sialendoscopy.....	40
5.0	Summary.....	41
6.0	References	42

Preface

Until recently, it was not possible to make a definitive diagnosis in a large percentage of patients with inflammatory and nonneoplastic swellings of the major salivary glands, despite the use of modern imaging

techniques. Salivary duct endoscopy (sialendoscopy) now closes this gap by allowing direct visualization of the ductal system. Moreover, constant advances are enabling us to provide therapeutic measures

through interventional sialendoscopy. This booklet explores the applications of sialendoscopy in obstructive diseases of the major salivary glands.

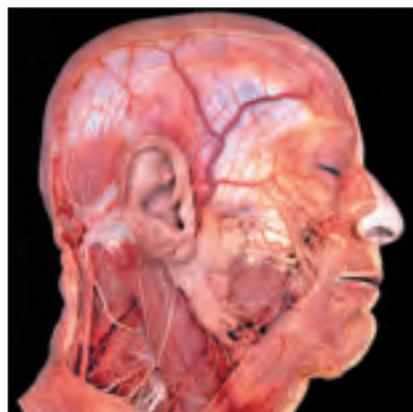


Fig. 1.1
Topography of the major salivary glands. The right parotid duct runs almost straight forward from the gland.

By courtesy of publishing house Schattauer GmbH, Stuttgart, Germany, from: *ROHEN JW, YOKOCHI C, LÜTJEN-DRECOLL E: Color Atlas of Anatomy. A Photographic Study of the Human Body, 6th edition 2006*

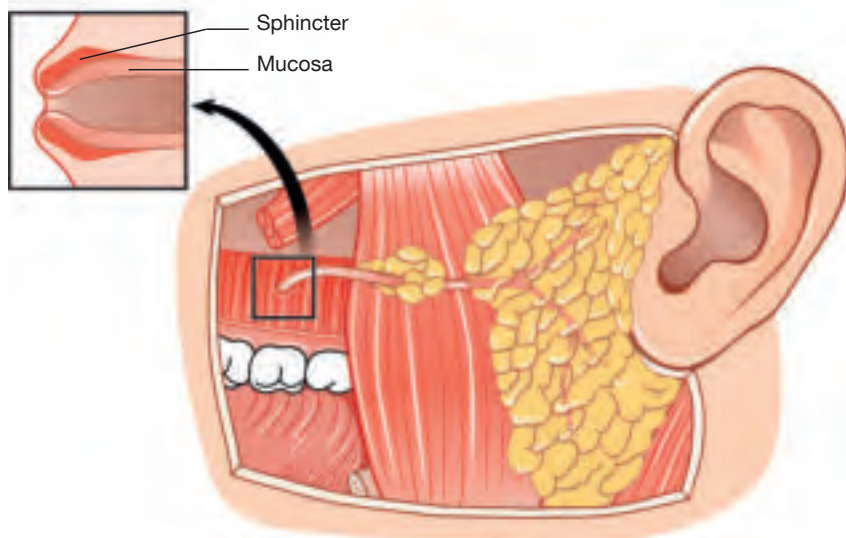


Fig. 1.2
Topographic anatomy of the parotid gland.

1.0 Anatomy of the Major Salivary Glands

Parotid Gland

The parotid gland is embedded in the retromandibular fossa between the vertical ramus of the mandible and the mastoid. Shaped like a transverse triangle, it is enclosed within a subcutaneous pseudocapsule. The gland is bounded anteriorly by the masseter muscle and mandible, and posteriorly by the sternocleidomastoid muscle and the posterior belly of the digastric muscle. Deep to the gland are the retromandibular vein and external carotid artery.

Parotid Duct (Stenon Duct)

The excretory duct of the parotid gland averages 6 cm in length and is formed by the confluence of second- and third-order tributary ducts. It leaves the gland in its anterosuperior third and runs forward over the masseter. It winds around the anterior border of that muscle to pierce the buccinator and buccal mucosa. The average diameter of the parotid duct is 1.4 mm at the hilum, 1.2 mm in its course through the buccinator, and 0.5 mm at the duct orifice.



Fig. 1.3
The orifice (arrow) of the right parotid gland is a small opening with raised circular edges located opposite the crown of the second upper molar.

Submandibular Duct (Wharton Duct)

The submandibular duct runs backward along the inferior border of the mylohyoid. On reaching the posterior border of that muscle, it turns upward at a 24–178° angle and runs forward along the medial side of the sublingual gland, opening on the sublingual papilla next to the frenulum of the tongue. The average diameter of the duct at its orifice is 0.5 mm.

The submandibular duct is surrounded throughout its course by glandular tissue, which belongs partly to the submandibular gland and partly to the sublingual gland. The excretory duct itself has an average diameter of 1.5 mm and is approximately 5–6 cm long. It crosses over the lingual nerve distal to the hilar region.

Sublingual Gland

The sublingual gland is located beneath the mucosa of the anterior floor of the mouth, directly overlying the mylohyoid. It relates laterally to the medial surface of the mandible

and the submandibular duct. Excretory ducts from the gland may drain into the submandibular duct, or smaller ducts may open directly into the mucosa of the oral floor.



Fig. 1.4
Topography of the right submandibular gland.

By courtesy of publishing house Schattauer GmbH, Stuttgart, Germany. from: ROHEN JW, YOKOCHI C, LÜTJEN-DRECOLL E: *Color Atlas of A Photographic Study of the Human Body*, 6th edition 2006

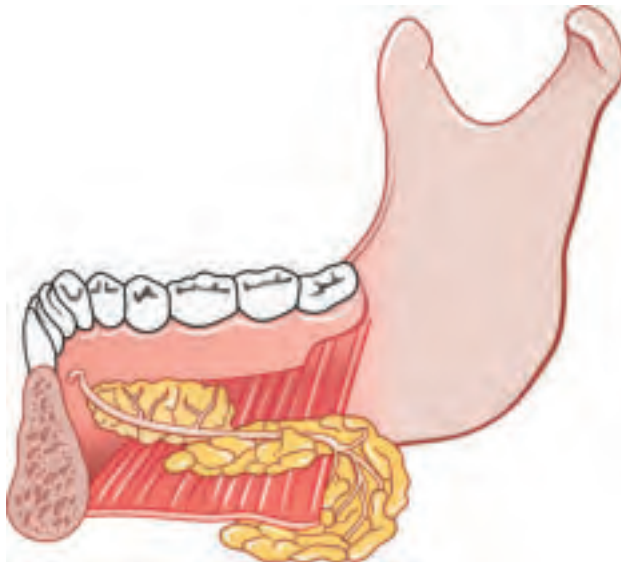


Fig. 1.5
Lateral view of the submandibular duct system.

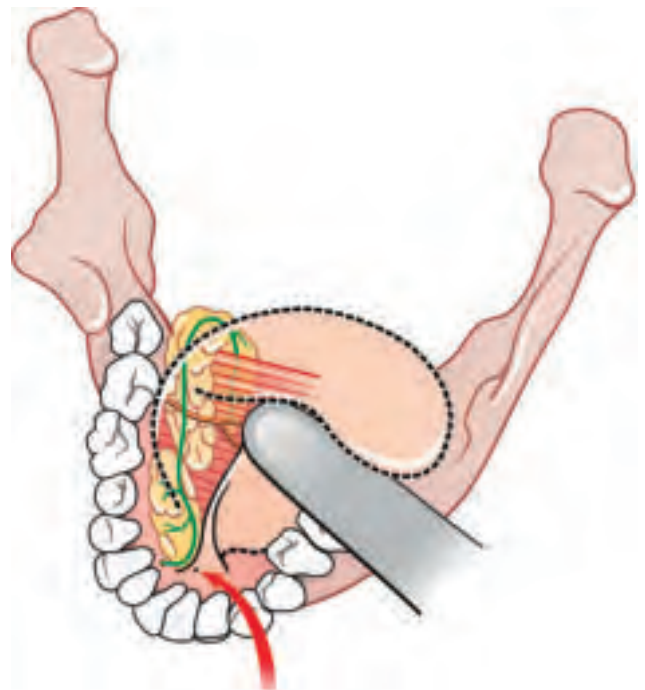


Fig. 1.6
Topography of the duct system of the submandibular gland. The submandibular duct opens on the sublingual papilla.

2.0 Diagnostic Imaging

High-Resolution B-Mode Ultrasonography

B-mode ultrasonography is the modality of first choice for salivary gland imaging at our institution. Ultrasound can differentiate inflammatory changes from neoplastic changes. While sonographic imaging of the glands themselves generally presents no difficulties, the excretory ducts cannot be visualized when in a healthy state—although segments of ducts can, sometimes be resolved with modern instruments.

Viewed in axial section, the parotid gland appears as a smooth-bordered organ of uniformly high echogenicity. The anterior portions of the gland overlie the masseter muscle and mandible. The posterior portion of the gland is located in the retromandibular fossa, bounded anteriorly by the mandible and posteriorly by the mastoid and sternocleidomastoid muscle. The posterior belly of

the digastric muscle, the internal carotid artery, and the internal jugular vein can be identified medial and caudal to the inferior pole of the parotid gland.

The submandibular gland curves around the posterior border of the mylohyoid and often extends anteromedially to the sublingual gland. The hyoid bone is occasionally projected into the submandibular compartment as a sonodense structure with a posterior acoustic shadow and should not be confused with a sialolith.

The submandibular gland appears sonographically as a hyperechoic structure with a homogeneous echo pattern. It has the same echogenicity as the parotid gland.

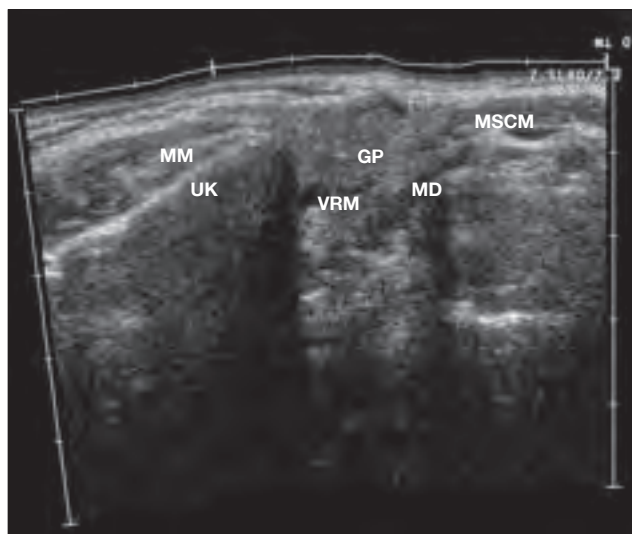


Fig. 2.1
Transverse scan of the left parotid gland with important landmarks indicated. **UK** = vertical ramus of mandible, **MM** = masseter muscle, **VRM** = retromandibular vein, **GP** = parotid gland, **MD** = posterior belly of digastric muscle, **MSCM** = sternocleidomastoid muscle.

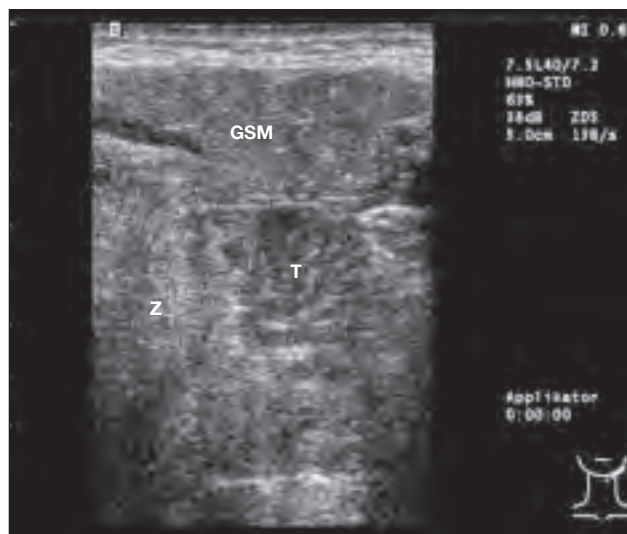


Fig. 2.2
Transverse scan in the left submandibular compartment shows the submandibular gland (**GSM**) in direct proximity to the palatine tonsil (**T**) and the tongue (**Z**). The hypoechoic structure of the mylohyoid is visible on the medial side.

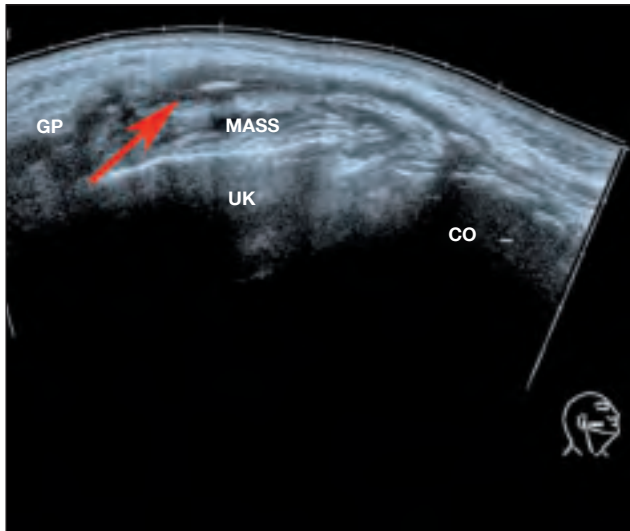


Fig. 2.3

Transverse scan of a right parotid gland with one stone near the hilum and a second stone near the duct orifice (**arrow**). The calculi appear as well-defined hyperechoic structures but show very little acoustic shadowing. The obstruction has caused dilatation of the duct and parotid gland (**GP**). **MASS** = masseter muscle, **UK** = mandible, **CO** = oral cavity.

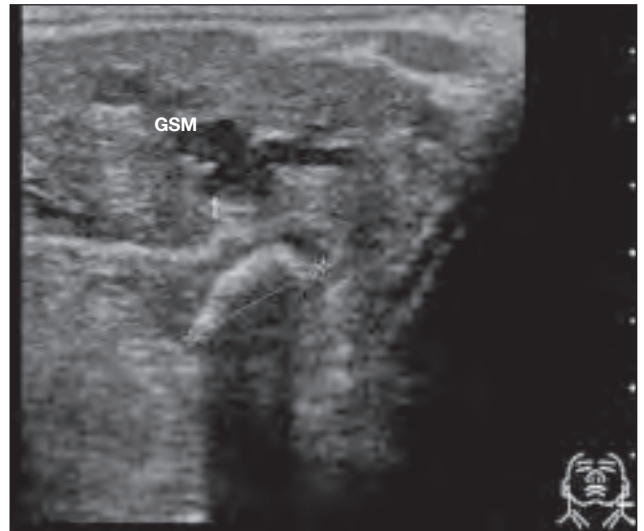


Fig. 2.4

Transverse scan in the left submandibular compartment demonstrates a stone in the hilar area of the submandibular gland (**GSM**). The proximal dilatation in the gland (**arrow**) is caused by an 11.2-mm echogenic stone with a posterior acoustic shadow (**cursors**).

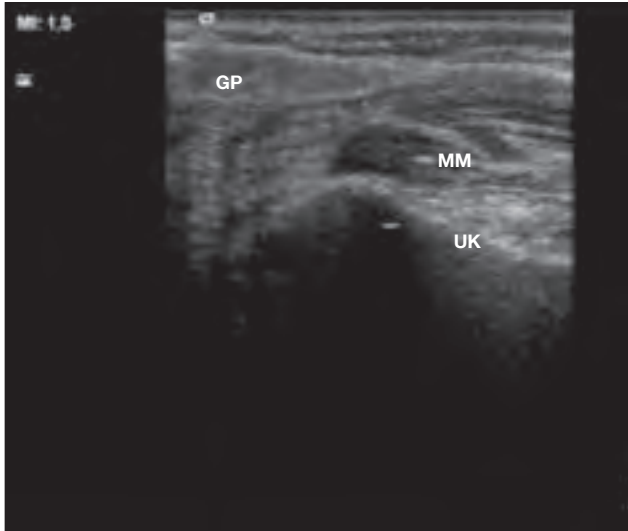
The echo texture of the glandular parenchyma can provide information on acute or chronic changes that occur in obstructive forms of sialadenitis. An enlarged parotid or submandibular gland with a coarsened, hypoechoic, nonhomogeneous, spongy echo texture and visible duct segments is characteristic of a florid obstructive disease. The sonographic appearance of chronic sialadenitis depends on the duration and extent of the parenchymal changes. Typical findings are a marked coarsening of the parenchymal echo texture and a nonhomogeneous internal echo pattern due to scarring and fibrosis. The parenchyma may also contain small cystic areas representing

circumscribed foci of ductectasia. Shrinkage of the gland relative to the opposite side, with or without obstructed ductal elements, suggests inflammatory or sclerotic atrophy of the gland over a period of years. Sialoliths appear sonographically as hyperechoic structures with distal acoustic shadowing, frequently accompanied by obstruction of the proximal duct system. While posterior acoustic shadowing is consistently present, occasionally the bright stone echo cannot be clearly seen due to scattering artifacts. Noncalcified obstructions occur at a site of ductal stenosis, and dilatation of the duct is not observed distal to the stenosis.



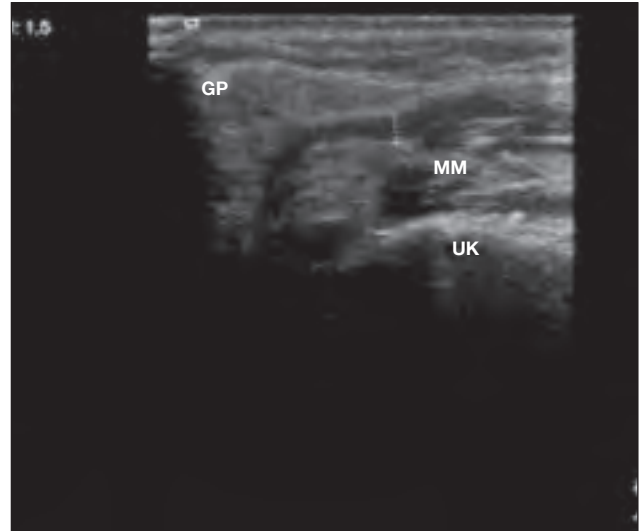
Fig. 2.5

Details on a millimeter scale can be defined with the use of high-resolution multifrequency transducers (Acuson Antares, Siemens Medical Solutions, Inc.).

**Fig. 2.6**

Chronic recurrent sialadenitis. The patient presented with recurrent periprandial swelling. Ultrasound shows slight proximal dilatation of the right parotid duct with no evidence of a sialolith.

MM = masseter muscle, **GP** = parotid gland, **UK** = mandible.

**Fig. 2.7**

Chronic recurrent sialadenitis. The imaging of obstructive dilatative changes can be improved by administering a sialagogue (here, ascorbic acid).

MM = masseter muscle, **GP** = parotid gland, **UK** = mandible.

Plain Radiographs

Conventional plain radiographs of the oral floor, submandibular gland, and parotid gland are rarely indicated because the glands are obscured by superimposed structures. Up to 50% of parotid duct stones and 20% of submandibular duct stones go undetected on plain radiographs, depending on their degree of mineralization.

**Fig. 2.8**

Opaque stones must be at least 2–3 mm in diameter to be visible on conventional radiographs. Submandibular duct stones near the ductal orifice may be obscured by the mandible and often cannot be reliably detected.

Sialography

Catheterization of the excretory ducts followed by the instillation of radiographic contrast medium can accurately define the ductal systems of the parotid and submandibular glands. This procedure is contraindicated in patients with acute inflammation due to the risk of complications (infection, abscess formation, extravasation). Conventional and digital-subtrac-

tion sialography can detect obstructions directly or indirectly in the form of filling defects (**Fig. 2.9**). Air inclusions may lead to false-positive findings. Possible indications in selected cases include the detection of very small stones in the excretory ducts, anomalies of the excretory ducts, sialadenosis, and chronic inflammatory processes.



Fig. 2.9
The stone (**arrow**) appears as a filling defect after catheterization and contrast injection.

MR Sialography

MR imaging of the salivary glands makes it possible not only to demonstrate ductal structures but also evaluate functional parameters of glandular activity (**Fig. 2.10**). The MR signal characteristics of the ducts are nonspecific, however. While current developments such as virtual salivary gland endoscopy

by MR sialography and 3D reconstructions can provide indirect visualization of the duct system, they do not allow for interventional procedures, and the relatively high costs of MRI make it less desirable than high-resolution ultrasound for routine imaging.

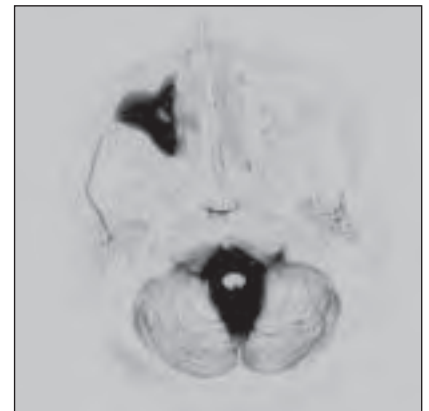


Fig. 2.10
MR sialogram (negative image) demonstrates the parotid duct on the right side.

3.0 Sialendoscopy

3.1 Prerequisites for Endoscopic Examination of the Major Salivary Ducts

To establish a basis for direct endoscopic examination of the excretory ducts of the major salivary glands (sialendoscopy), we first had to make an accurate determination of duct dimensions. Studies indicated that the parotid and submandibular ducts each had an average diameter of 1.5 mm. The parotid duct

orifice had an average diameter of 0.5 mm, and the submandibular duct orifice measured approximately 0.1–0.5 mm. This showed that endoscopes with an outer diameter of up to 1.7 mm would be suitable for evaluating the excretory ducts of the major salivary glands. The narrow duct orifice must be

passable for the endoscope, and generally this requires expanding the orifice with a dilatator. Given the scant amount of muscle in the duct walls, the studies showed that continuous irrigation of the duct system is necessary to maintain luminal distension and keep the walls from collapsing.

3.2 Instruments and Endoscopes

The earliest descriptions of flexible endoscopes for salivary duct examination were published by *Königsberger* in 1990 and *Katz* in 1991. These endoscopes caused minimal trauma owing to their small diameter and flexibility, but image quality was unsatisfactory due to their poor optical properties and the absence of an irrigation channel in many sialendoscopes. Rigid endoscopes provided better optical quality but caused

greater trauma to the duct epithelium. Today, semirigid or semiflexible endoscopes have become standard for sialendoscopy. These endoscopes have a smooth, flexible, atraumatic shaft. Modern sialendoscopes with an outer diameter of up to 1.7 mm are excellently suited for all major salivary ducts. The technical advances to date are reviewed in **Tab. 1**:

Tab. 1: Technical Advances in Salivary Duct Endoscopy

	Endoscope	Diameter of endoscope	Diameter of working channel	Diameter of irrigation channel
<i>Königsberger</i> 1990	Flexible	————	————	————
<i>Katz</i> 1991	Flexible	0.8 mm	————	————
<i>Gundlach</i> 1994	Flexible	2.0 mm	0.6 mm	————
<i>Nahlieli</i> 1994	Rigid	2.7 mm	————	————
<i>Iro</i> 1995	Flexible	1.6 mm	0.6 mm	————
<i>Iro</i> 1996	Flexible	1.5 mm	0.2 mm	————
<i>Arzoz</i> 1996	Rigid	2.1 mm	1.0 mm	————
<i>Yuasa</i> 1997	Rigid/flexible Rigid/flexible	0.8 mm 1.0 mm	———— ————	———— ————
<i>Marchal</i> 1997	Flexible	1.5 mm	0.5 mm	————
<i>Yuasa</i> 1997	Rigid/flexible	0.8 mm, 1.8 mm	————	————
<i>Nahlieli</i> 1997	Rigid Rigid	2.0 mm 2.5 mm	———— 1.0 mm	———— ————
<i>Marchal</i> 1998	Semiflexible Semiflexible	1.3 mm 2.67 mm ²	0.8 mm 0.8 mm	———— ————
<i>Nahlieli</i> 1999	Semiflexible Semiflexible	1.3 mm 2.3 mm x 1.3 mm	1.0 mm 1.0 mm	———— Yes
<i>Iro</i> 2000	Semiflexible	1.1 mm 1.2 mm	0.4 mm 0.6 mm	———— Yes
<i>Marchal</i> 2001 und 2002	Semiflexible Semiflexible	1.3 mm 2.29 mm ²	0.8 mm 0.8 mm	Yes
<i>Zenk</i> 2004	Semiflexible	1,1 mm	0.4 mm	Yes
<i>Erlangen</i> 2004/2007	Semiflexible Semiflexible Semiflexible	0.8 mm 1.1 mm 1.6 mm	0.25 mm 0.4 mm 0.8 mm	———— 0.25 mm 0.25 mm

3.3 The Erlangen Endoscopy Set

In recent years we have developed an endoscopic instrument set based on our own clinical experience and basic research (KARL STORZ Tuttlingen, Germany). Each endoscope is equipped with an irrigation channel to provide luminal distension and improve the visualization of findings. Several endoscopes are supplied in the set. A basic distinction is made between endoscopes for diagnostic purposes (irrigation channel only) and endoscopes for diagnostic **and** interventional procedures (irrigation channel plus working channel). The image transmission system has a resolution of up to 10,000 pixels. The fiber optic light cable with coupled endoscope can be connected to a standard cold light source and video system. Alternatively, the

surgeon may look directly through an eyepiece. All the endoscopes can be treated with standard disinfectant solution or gas/plasma sterilization.

The semiflexible endoscopes provide a 0° straight forward angle of view. The eyepiece is offset, with a built-in fiber optic light cable, 140 cm in length. The endoscopes have an outer shaft made of Nitinol to provide adequate flexibility. The working length is 10 cm, with calibration markings at 1-cm intervals along the shaft.

The diagnostic endoscope has an outer diameter of 0.8 mm and a 0.25-mm irrigation channel (**Figs. 3.2 and 3.3b**).



Fig. 3.1
Overall view of the Erlangen endoscopy set.



Fig. 3.2
Semiflexible sialendoscope with centimeter markings.



Fig. 3.3a
Sialendoscope for diagnostic purposes.

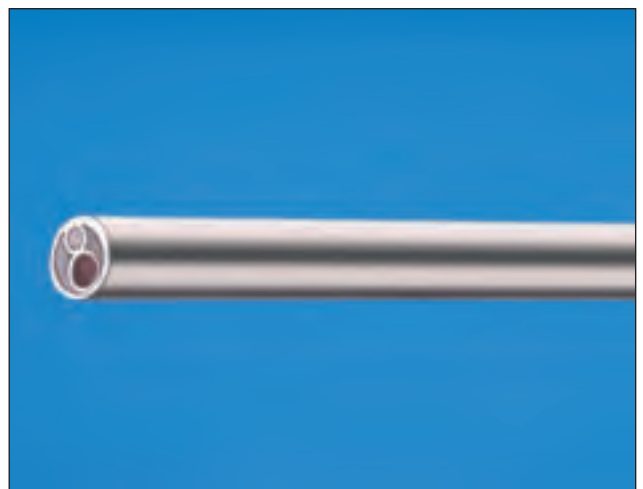


Fig. 3.3b
Distal tip of the diagnostic sialendoscope with irrigation channel.

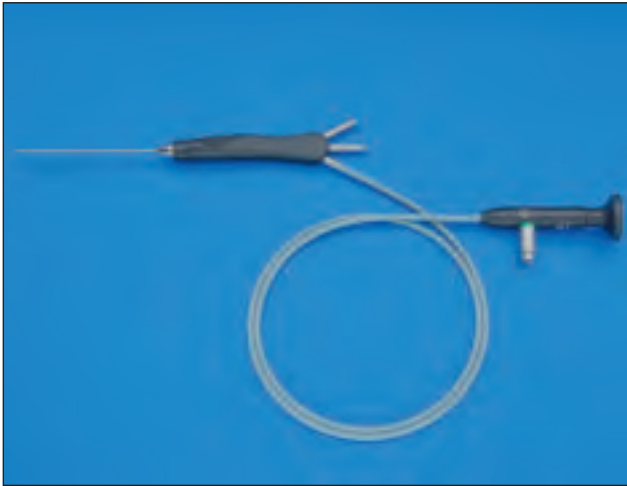
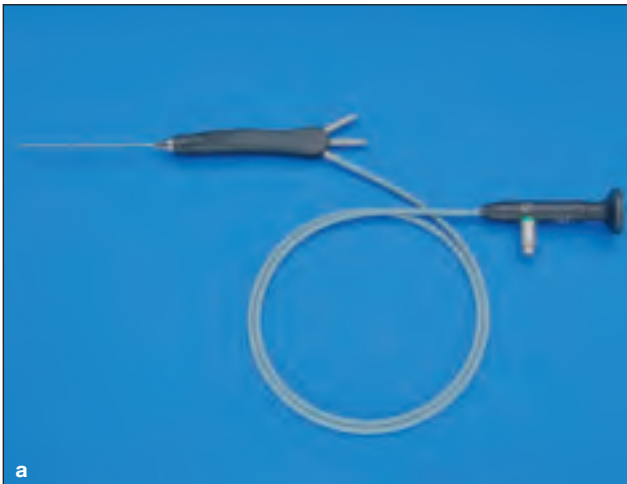


Fig. 3.4
Endoscope for interventional therapy. The outer diameter is 1.1 mm.

Two endoscopes are available for interventional therapy. One has an outer diameter of 1.1 mm, a 0.25-mm irrigation channel, and a 0.45 mm-working channel (**Fig. 3.4**).

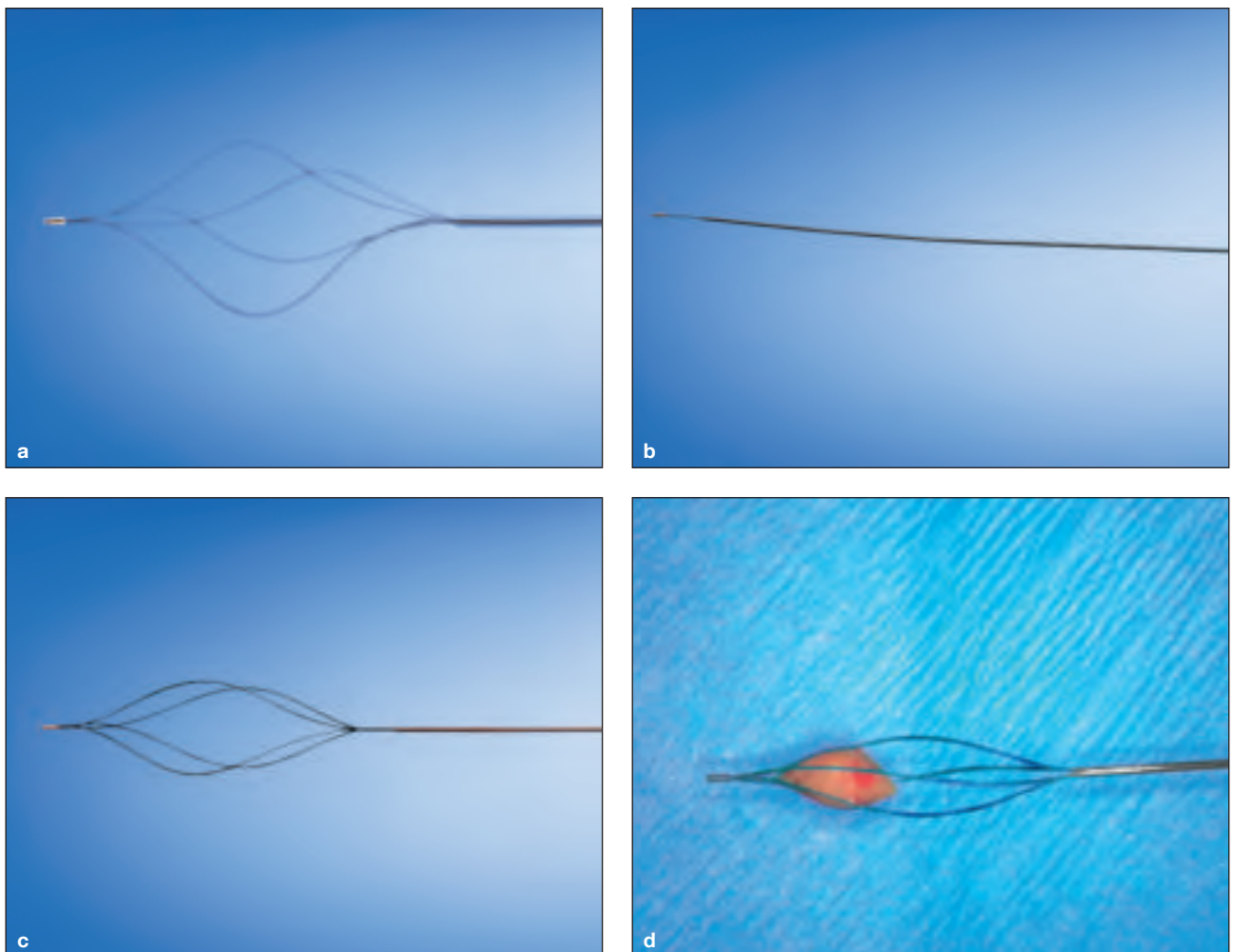
The second endoscope has an outer diameter of 1.6 mm, a 0.25 mm-irrigation channel, and a working channel of 0.8 mm (**Fig. 3.5b**).



◀ **Figs. 3.5a–c**
Endoscope for interventional therapy, with an outer diameter of 1.6 mm (**a**). Proximal-end view shows the optical channel and two additional channels – the smaller irrigation channel and larger working channel for operating instruments (**b**). View with an instrument in the working channel (**c**).

Various instruments ranging from 0.38 to 0.8 mm in diameter are available for use through the instrument channel (Figs. 3.5 and 3.6). The following are among the most important instruments for transendoscopic use:

Wire basket: has four wires and an outer diameter of 0.4 mm. The basket is opened and closed by manipulating a handle. It is useful for extracting stones, plaques, and foreign bodies. The object should be mobile rather than impacted so that the tip of the basket can be maneuvered past it for retrieval.



Figs. 3.6a–d
Wire basket (a), in the closed position (b), open position (c), and with a stone ready for extraction (d).



Fig. 3.7
Grasping forceps.

Grasping forceps: flexible with an outer diameter of 0.78 mm and working length of 30 cm. The double-action jaws have a serrated grasping surface. If the stone is not too large, it can be extracted in one piece. If its consistency is not too hard, the stone can be fragmented with the forceps for piecemeal removal. This instrument can also be used for foreign body retrieval.



Fig. 3.8
Biopsy forceps.

Biopsy forceps: has an outer diameter of 0.78 mm. Both jaws are movable and have sharp cutting edges. These properties also make the forceps suitable for excisional biopsies.

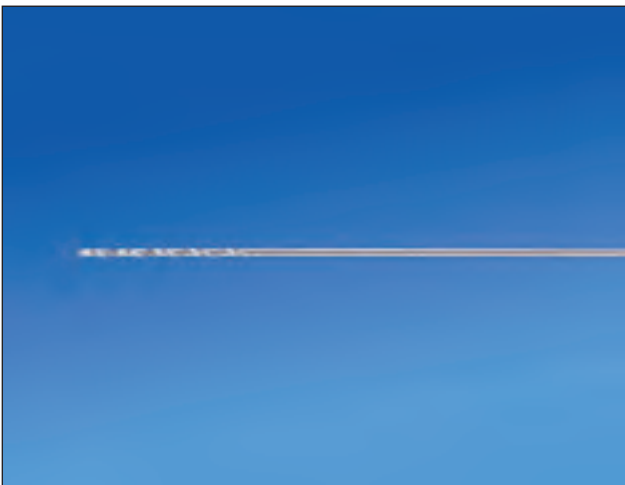


Fig. 3.9
Micro burr.

Micro burr: measures 0.38 mm in diameter. Can be used to reduce or fragment stones prior to extraction, particularly stones not amenable to primary basket retrieval. The sharp edges of the burr are also useful for opening filiform or complete stenoses. The burr can restore an absent lumen or expand a small residual lumen to permit insertion of other instruments such as a wire basket or balloon.

3.4 Technique of Salivary Duct Endoscopy

Salivary duct endoscopy can generally be performed under local anesthesia. First the oral mucosa is anesthetized with a topical spray (e.g., 2% lidocaine spray).

Then the papilla is dilated (Figs.

3.11 and 3.12). This is performed with the tapered conical tip of a salivary duct dilator 14 cm long (Fig. 3.10). Assorted tip widths are available so that even very narrow orifices can be dilated (Figs. 3.12).

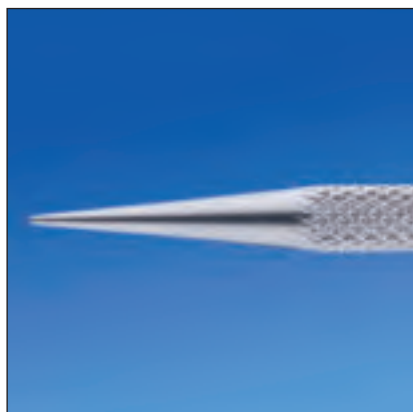


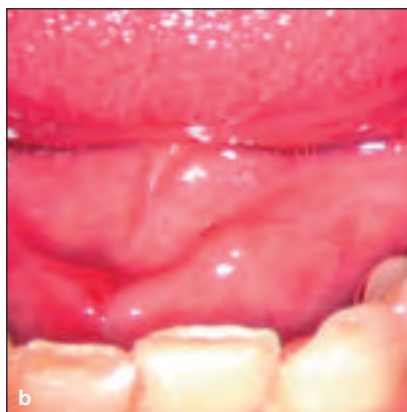
Fig. 3.10
Dilatator with tapered conical tip.



Figs. 3.11a, b
Dilation of the parotid duct orifice.



Figs. 3.12a, b
Dilation of the submandibular duct orifice.



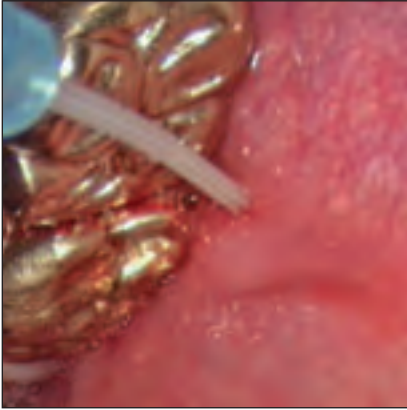
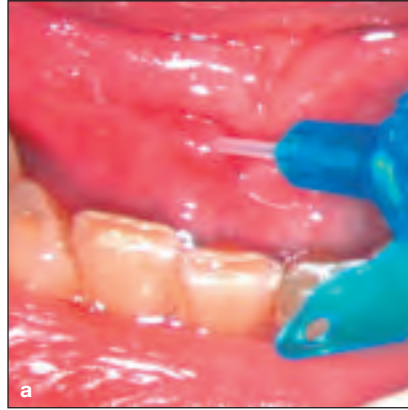


Fig. 3.13
Intraductal anesthesia of the parotid duct system.



Figs. 3.14a, b
Intraductal anesthesia of the submandibular duct (a) and introduction of the endoscope (b).



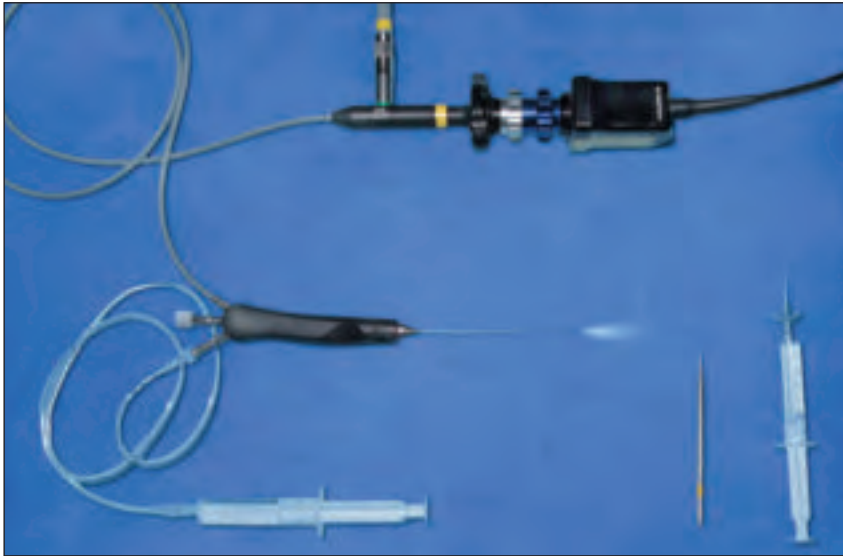
Fig. 3.15
Papillotomy at the caruncle (view through the endoscope prior to insertion; pointer highlights the papilla).

Next, a local anesthetic solution (e.g., 2% carticaine) is injected into the duct through an indwelling venous catheter (22 gauge, 0.9 mm) (**Figs. 3.13** and **3.14a**). Besides anesthetizing the duct, the solution will also relax the intra- and periductal musculature to facilitate insertion of the endoscope (**Fig. 3.14 b**).

Using the technique described above, sialendoscopy can be successfully performed in the majority of cases. Rarely, introduction of the endoscope may be difficult or

impossible due to various causes (extremely small duct orifice, papillary hypertrophy, papillary stenosis due to inflammation or scarring, small impacted stone). These cases will require a 3- to 4-mm mini-papillotomy incision or distal duct incision to permit insertion of the scope (**Fig. 3.15**).

Effective sialendoscopy requires continuous irrigation. This is accomplished with a syringe and tubing system connected to the endoscope.



◀ **Fig. 3.16**
Table setup for sialendoscopy.

Irrigation is necessary to overcome the sphincter-like contractile mechanism that keeps the duct in a collapsed state. Irrigation maintains adequate luminal distension so that intraductal structures and pathologic changes can be clearly visualized (**Figs. 3.18a, b**). In the absence

of obstructions, the sialendoscope can be advanced across the hilum into second- and third-order ducts. Problem areas are encountered where the parotid duct angles to pierce the buccinator muscle and in the “comma area” of the submandibular duct at the posterior

border of the mylohyoid. Assistants are needed for maintenance of continuous suction-irrigation and for handling the instruments. Diagnostic sialendoscopy generally lasts 10–25 minutes, while interventional procedures last from 20 to 60 minutes.

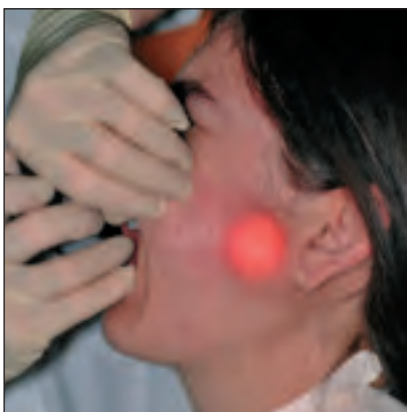
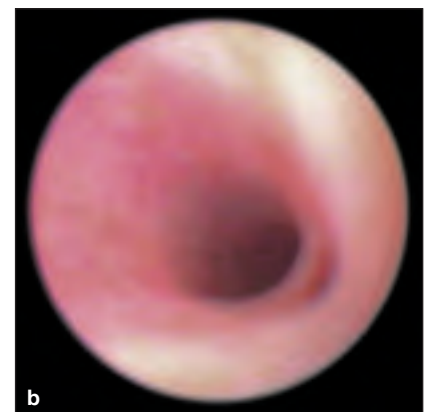
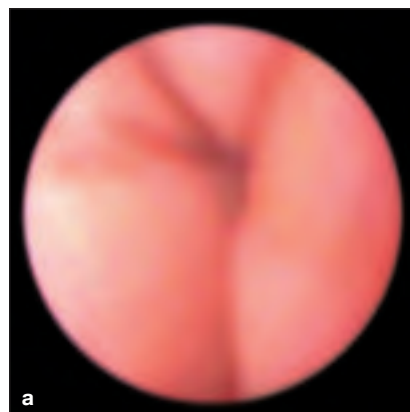


Fig. 3.17
Sialendoscopy of the parotid gland. Transillumination clearly indicates the position of the endoscope in relation to the gland.



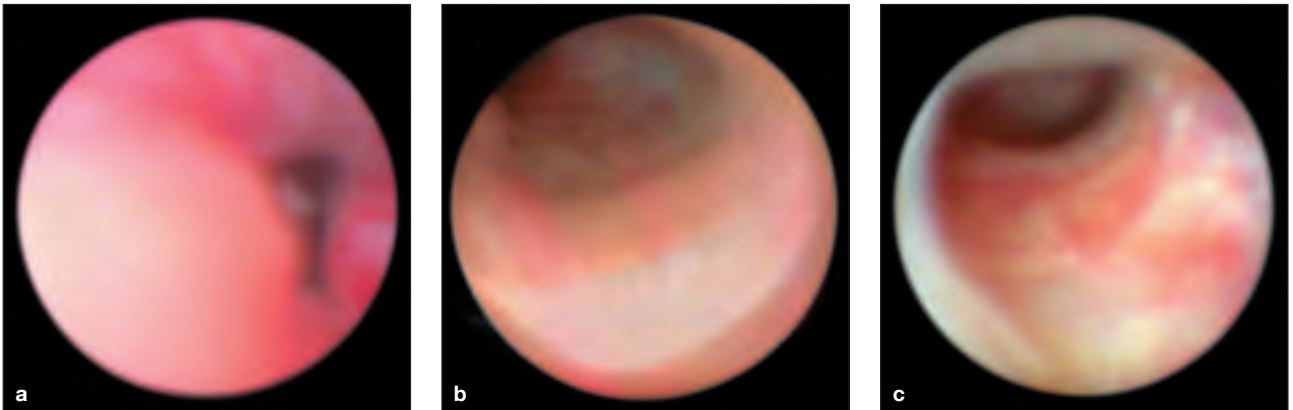
Figs. 3.18a, b
Collapsed duct lumen without irrigation (**a**) and luminal distension by irrigation (**b**).

3.5 Normal Findings in Sialendoscopy

Papillary Region

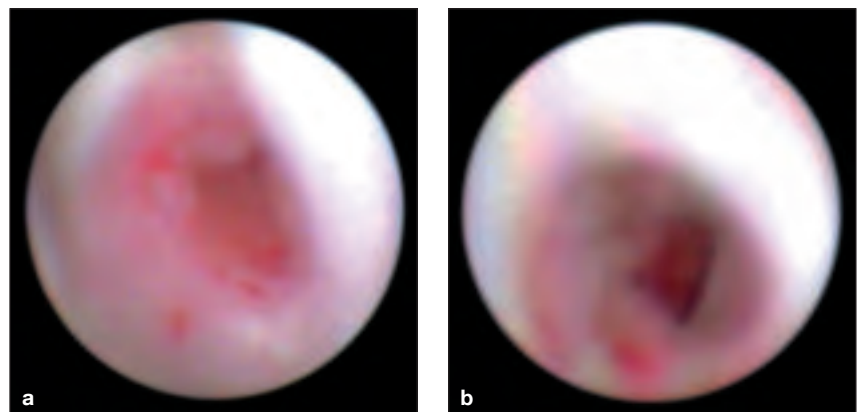
The papilla appears as a conical or crater-shaped elevation of the mucosa. The orifice of the submandibular duct is 0.1–0.5 mm in diameter, while the parotid duct orifice is slightly larger with an

average diameter of approximately 0.5 mm. The duct lumen tapers toward the orifice due to the presence of distal musculature (**Figs. 3.19** and **3.20**).



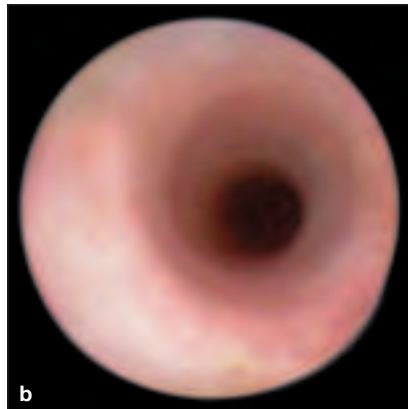
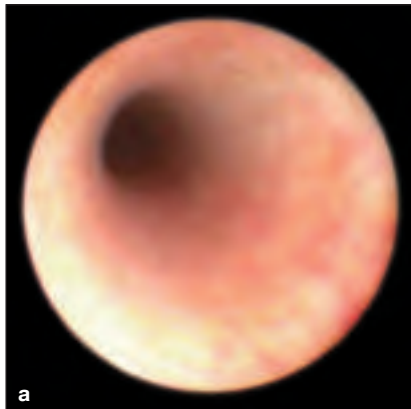
Figs. 3.19a–c

Papilla of the submandibular duct appears as a crater-shaped elevation in the mucosa (**a**). The tip of the endoscope has passed through the papilla (**b**). Conical taper of the prepapillary duct (**c**).



Figs. 3.20a, b

Papillary region of the parotid duct (**a**). The tip of the endoscope has passed through the papilla (**b**).



Figs. 3.21a, b
Main duct of the submandibular gland (a) and parotid gland (b).



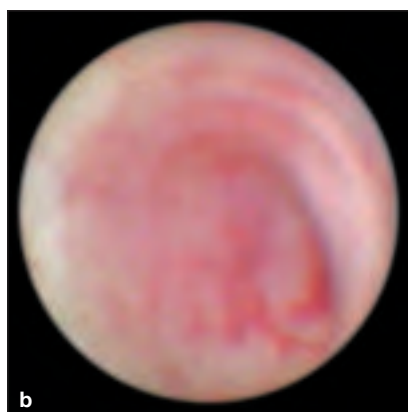
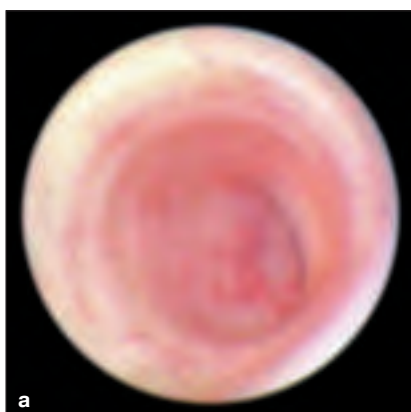
Fig. 3.22
Angled portion ("comma area") of the submandibular duct.

Main Duct

The normal salivary duct runs a straight course and presents a smooth, slightly pale to pink inner surface with a flat epithelial lining. Blood vessels are consistently visible through the duct epithelium. The healthy duct wall also presents faint circular ridges, which may reflect the sphincter-like mechanism of the periductal muscula-

ture (see **Figs. 3.18**) and are most prominent in the papillary region. Variable accessory ducts may branch from the main duct. Important regions are the "comma area" of the submandibular duct and the site where the parotid duct pierces the buccinator, as these areas may be difficult to surmount with the endoscope.

At the site where the parotid duct pierces the buccinator, the lumen becomes markedly narrowed as the duct makes an almost 90° posterior turn toward the masseter muscle (**Figs. 3.23a–c**).

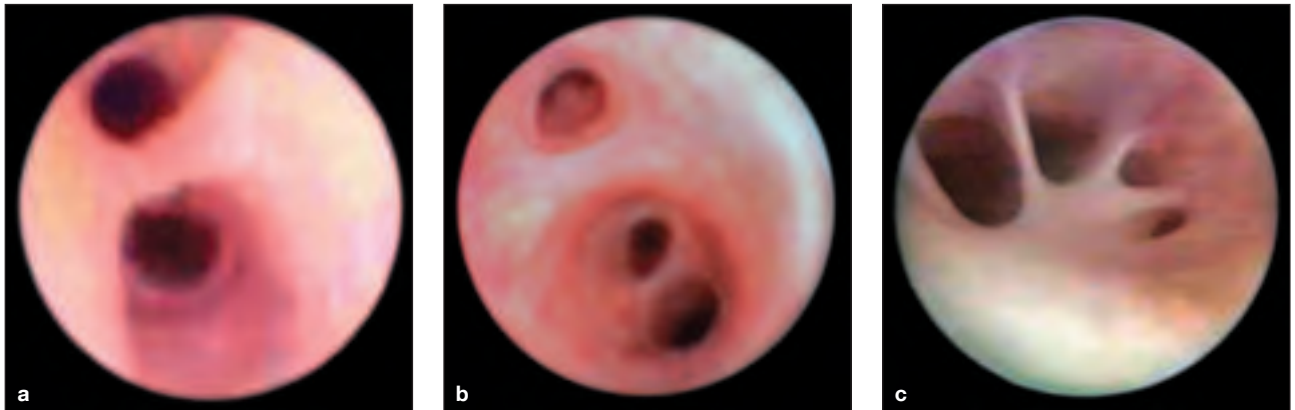


Figs. 3.23a–c
Passage of the parotid duct through the buccinator. The duct enters the muscle (a), narrows in its passage through the muscle (b), and emerges from the buccinator region (c).

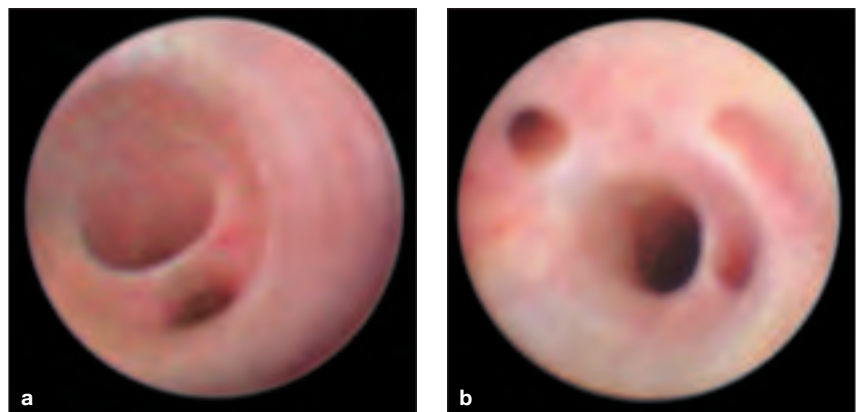
Hilar Region

The hilar region shows a highly variable pattern of duct branching. A bifurcation pattern is the most common, but other patterns may

be seen ranging from trifurcation to a multibranched configuration that resembles the renal pelvis (**Figs. 3.24** and **3.25**).



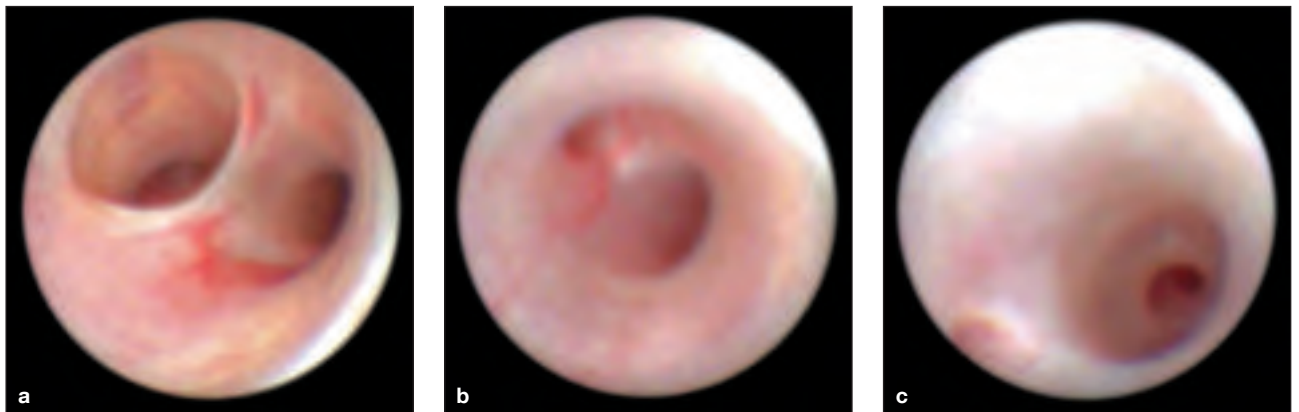
Figs. 3.24a–c
Hilar anatomy of the submandibular gland: bifurcation (**a**), trifurcation (**b**), and “renal pelvic” configuration with multiple branches (**c**).



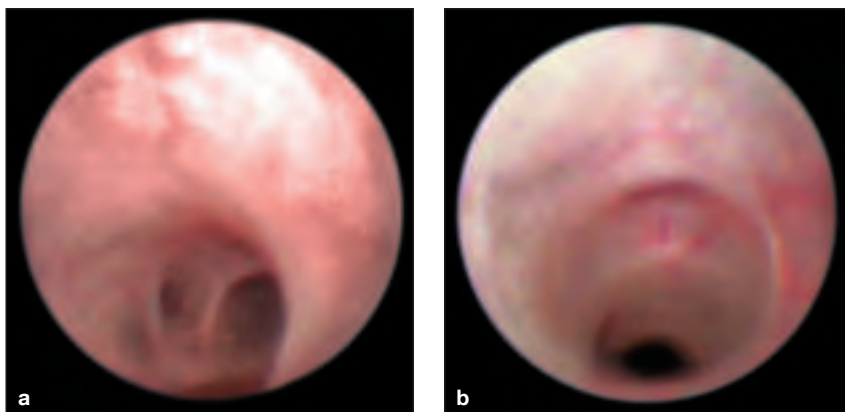
Figs. 3.25a, b
Hilar anatomy of the parotid gland: bifurcation (**a**) and multiple branches (**b**).

Intraparenchymal Duct System

Commonly, the posthilar area can be visualized by sialendoscopy as far as the second-order and third-order ducts.



Figs. 3.26a–c
Intraparenchymal posthilar duct system of the submandibular gland: second-order (a) and third-order ducts (c).



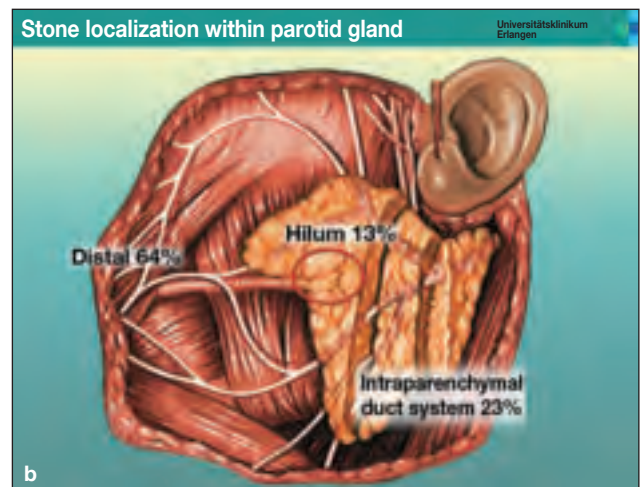
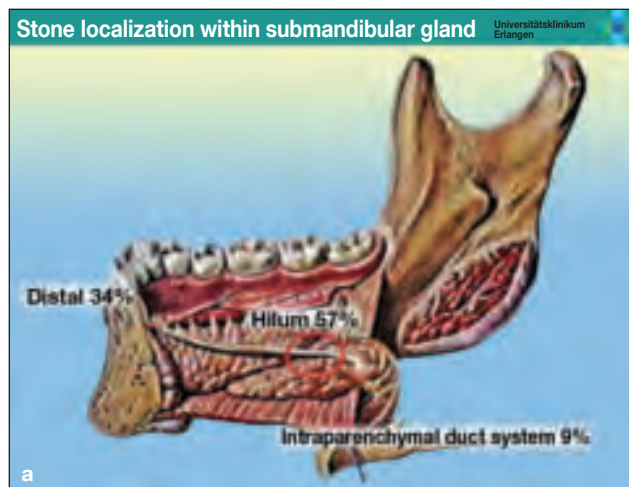
Figs. 3.27a, b
Intraparenchymal posthilar duct system of the parotid gland: second-order (a) and third-order ducts (b).

4.0 Diagnostic and Interventional Sialendoscopy in Various Diseases

4.1 Sialolithiasis

Sialolithiasis is a disease that predominantly affects adults and is twice as common in males. The peak age of occurrence is from 20 to 40 years. Sialolithiasis requiring treatment has a reported incidence of 30–60 per million population. An association with other biliary or urinary stone diseases has not been reported. Sialoliths are classified by their location as intraglandular or

extraglandular. Even intraglandular stones are generally intraductal and accessible to sialendoscopy. The submandibular gland is affected in 63–94% of cases, the parotid gland in 6–21%, and the sublingual gland in up to 16% of cases. Stones are very rarely encountered in the minor salivary glands (0.23% to 2% of all cases) (**Figs. 4.1a, b**).



Figs. 4.1a, b
Location and frequency of stones in submandibular and parotid gland.

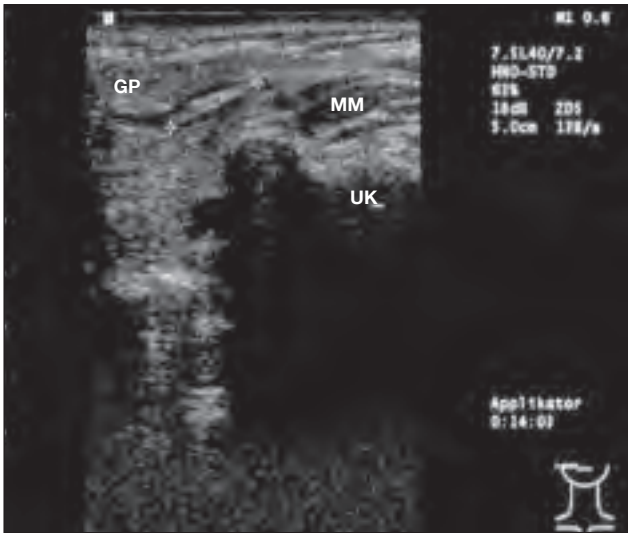


Fig. 4.2
 Transverse scan of the right parotid gland demonstrates a stone (10.8 mm, cursors) in the hilum. **GP** = parotid gland, **MM** = masseter muscle, **UK** = mandible.



Fig. 4.3
 Stone (8.7 mm, cursors) in the ostial region of the submandibular duct (**DW**), which is expanded to 7.3 mm (**cursors**). Closely adjacent to the stone and duct is the sublingual gland (**GSL**).

Primary ultrasound examination is indicated in all patients with obstructive sialadenitis. Ultrasound can confirm suspicion of sialolithiasis in the great majority of cases (**Figs. 4.2–4.4**).

In rare cases (stones < 1.5 mm and “soft” stones with

scant mineralization), the stone cannot be visualized with ultrasound. Over 20% of endoscopies performed in patients with unexplained salivary gland swelling can detect stones that were missed in previous imaging studies (**Fig. 4.5**).



Fig. 4.4
 Stone close to the duct orifice (**arrow**). Because of the obstructing stone, the entire parotid duct (**DUCT**) is visible in its course over the masseter muscle, mandible (**UK**), and in the parotid gland (**GP**), which is also dilated.

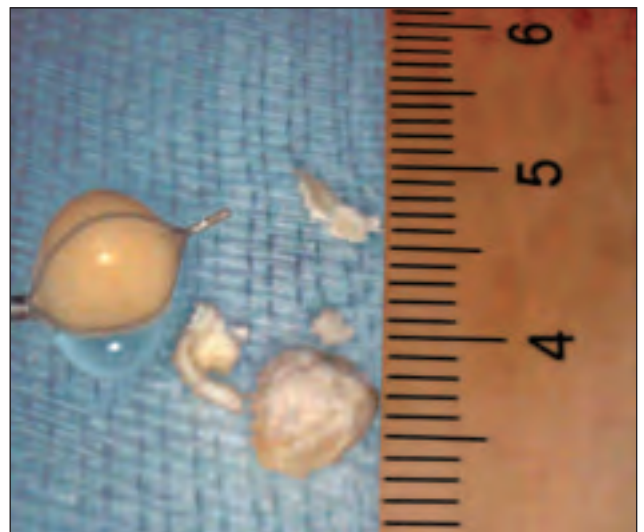


Fig. 4.5
 Left: stone of hard consistency (clearly visible at ultrasound) enclosed in a wire basket. Right: stone of soft consistency (difficult to detect at ultrasound).

Endoscopy of the duct system can detect a stone and determine its precise location in patients with clinical suspicion of sialolithiasis or a sonographically confirmed diagnosis. An important consideration in treatment planning is the question of whether the stone is located in the main duct, adjacent to or in the hilar region, or at a more proximal site in a second- or third-order

duct. Another important issue is the relationship of the stone to the duct wall, particularly whether the stone is mobile or impacted.

If the stone is accessible by endoscopy, not too large (5 mm) and is mobile, endoscopically controlled removal with various instruments is successful in up to 80% of cases. If a stone cannot be removed endoscopically with a basket, forceps,

or burr, a differentiated approach should be taken that depends on the location and the affected gland. If extracorporeal shock-wave lithotripsy (ESWL) has been performed, sialendoscopy is used to evaluate the degree of stone fragmentation and, if possible, complete the stone removal endoscopically.



Fig. 4.6
Mobile stone in the hilum.



Fig. 4.7
Mobile stone in the main duct just distal to the hilum.

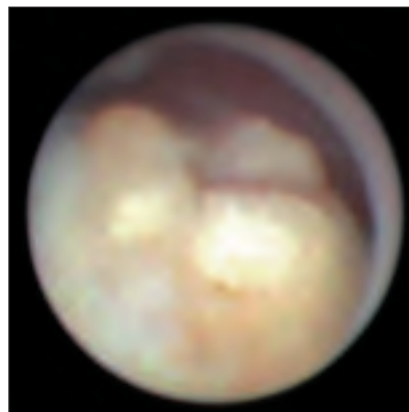


Fig. 4.8
Stone impacted in the hilum.



Fig. 4.9
Stone fragments after ESWL.



Fig. 4.10
Stone in the submandibular duct.

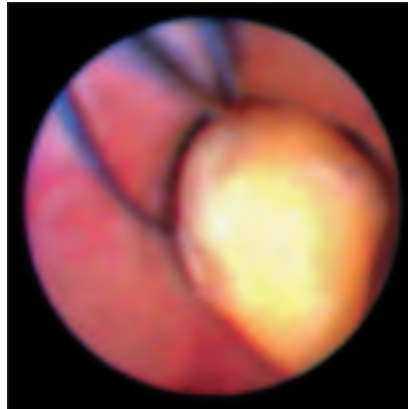
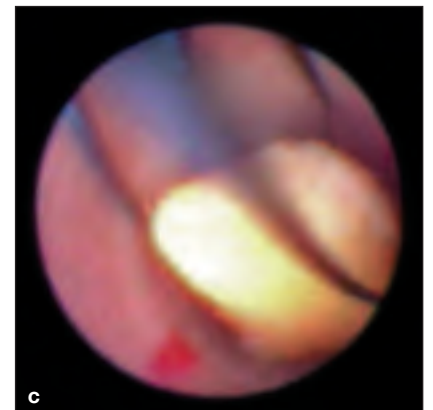
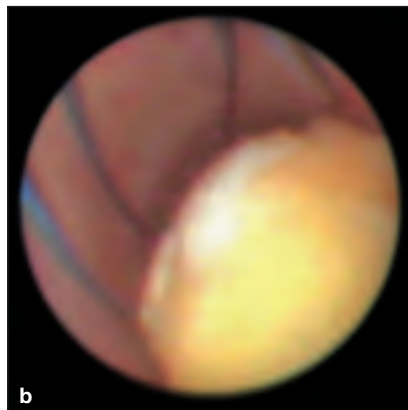
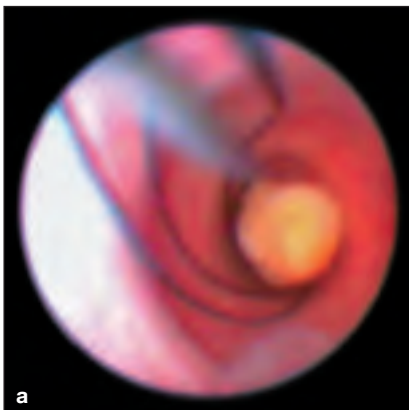


Fig. 4.11
For a basket extraction, it must be possible to advance the tip of the basket past the intraductal stone. This is possible only with mobile stones.

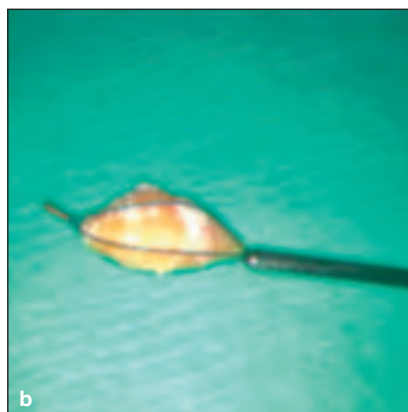
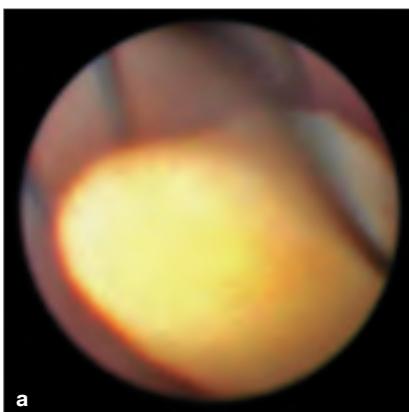
Examples of Therapeutic Sialendoscopy:

Basket Extraction of Stones

Primary submandibular stone removal with the wire basket.



Figs. 4.12a–c
The instrument is manipulated (a) to maneuver the stone into the basket (b) until it is encompassed by the wires (c).



Figs. 4.13a, b
The stone is trapped in the basket (a) and can be extracted (b).

Primary Parotid Stone Removal with the Wire Basket

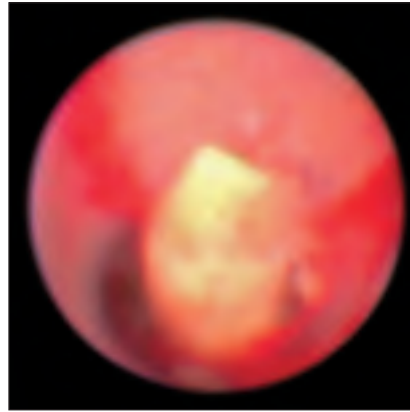


Fig. 4.14
Mobile stone in the main duct of the parotid gland.

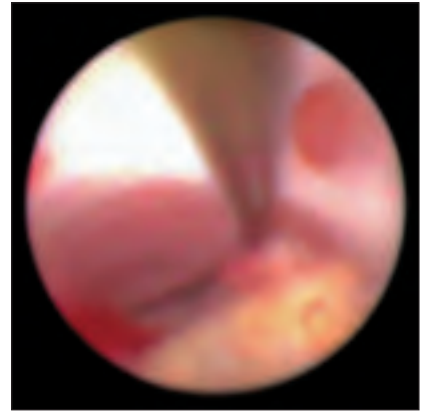
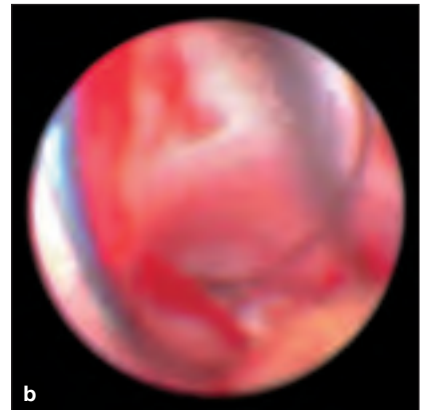
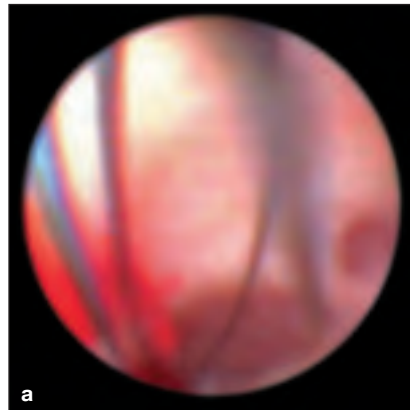
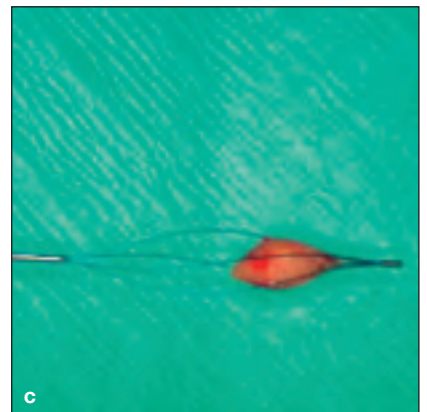
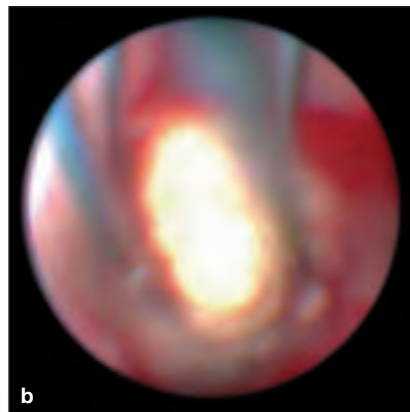
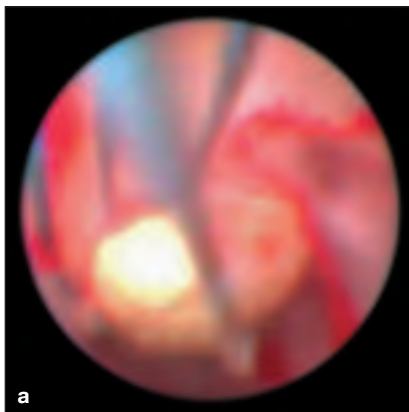


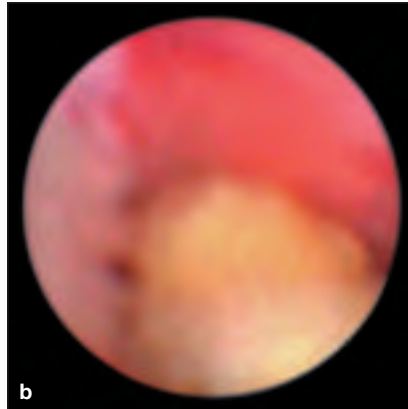
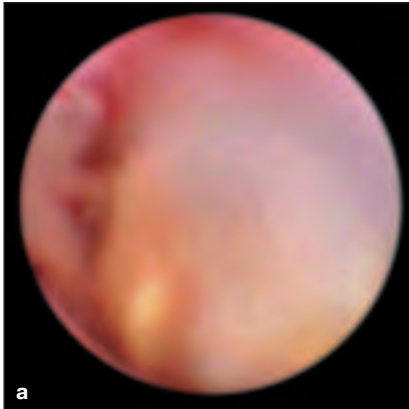
Fig. 4.15
The tip of the basket is maneuvered past the stone.



Figs. 4.16a, b
The basket is opened (a) so that the wires encompass the stone (b).



Figs. 4.17a–c
Stone is trapped in the basket (a) and extracted (b). Stone in the basket following extraction (c).



Intraductal Parotid Stone Fragmentation with the Micro Burr

Stones that cannot be removed primarily must be fragmented before extraction.

Figs. 4.18a, b

This stone in the parotid duct is less mobile and too large for primary basket extraction.



Fig. 4.19

The stone is progressively reduced in size with the micro burr.

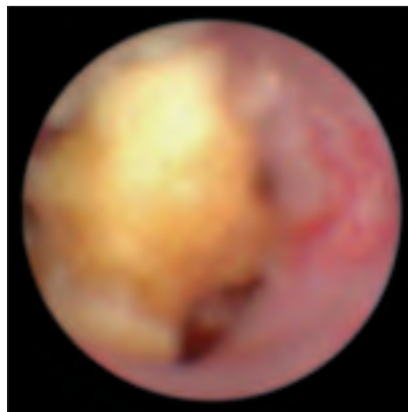
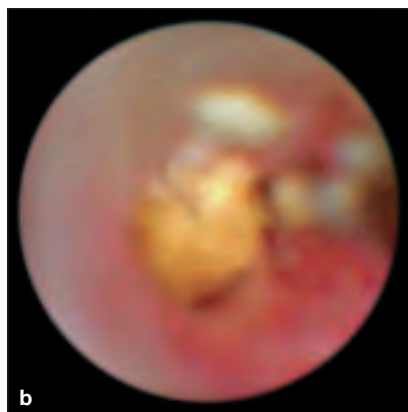
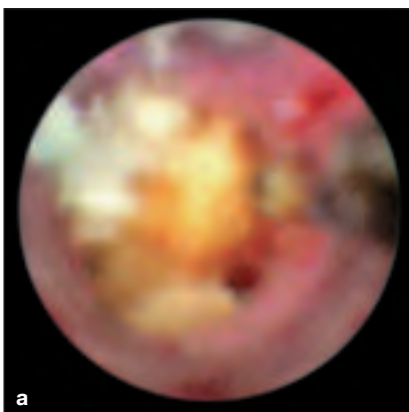


Fig. 4.20

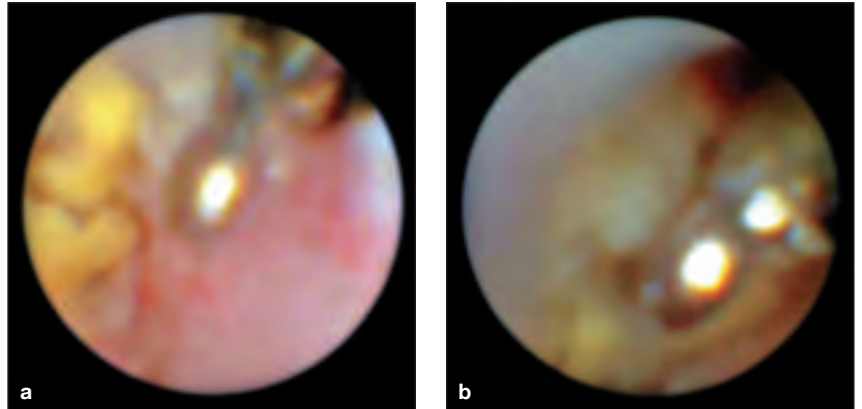
The stone is considerably more mobile.



Figs. 4.21a–c

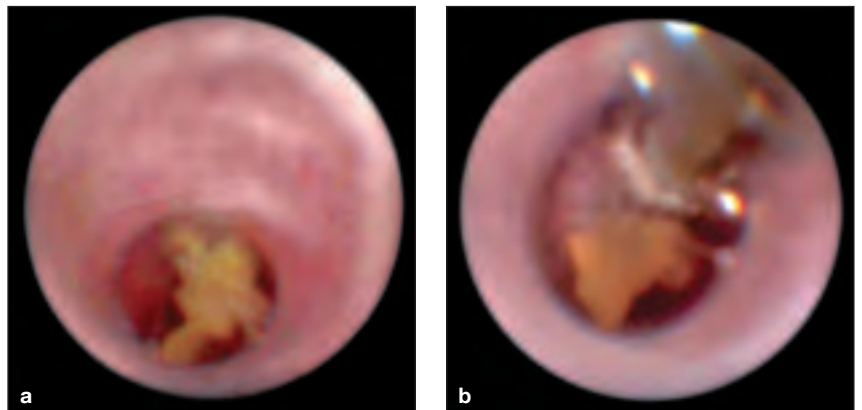
After further fragmentation, the residual stone is small enough for basket extraction.

Stone Fragmentation and Removal from the Parotid Duct with the Forceps



Figs. 4.22a, b

Stones that are too large, immobile, or impacted should be fragmented before extraction. Various endoscopic forceps are available for this purpose.



Figs. 4.23a, b

The fragments can be removed with the forceps or basket, or small fragments can be left alone to pass spontaneously.

Extracorporeal Fragmentation of Stones and Residual Fragments

If primary endoscopic removal fails, extracorporeal shock-wave lithotripsy (ESWL) can be attempted in an effort to reduce the stones to components that can be extracted endoscopically.

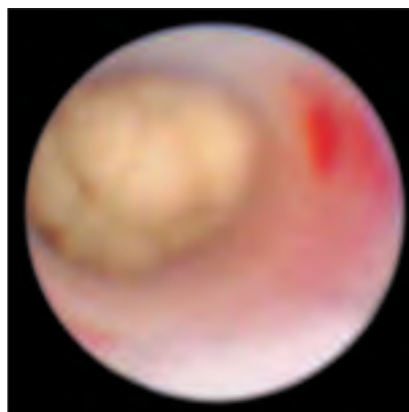


Fig. 4.24

Stone in the parotid duct following ESWL. The fissures in the stone are clearly visible.

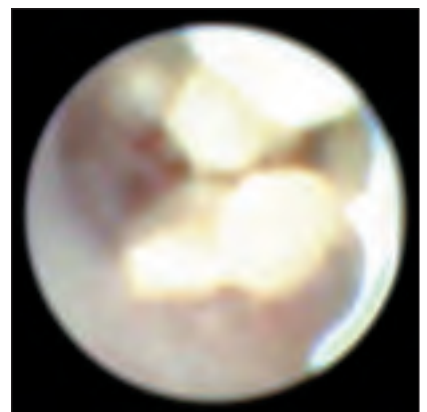
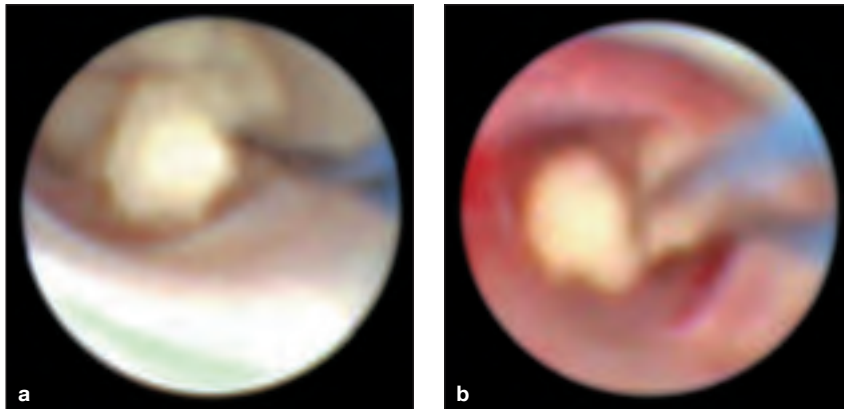


Fig. 4.25

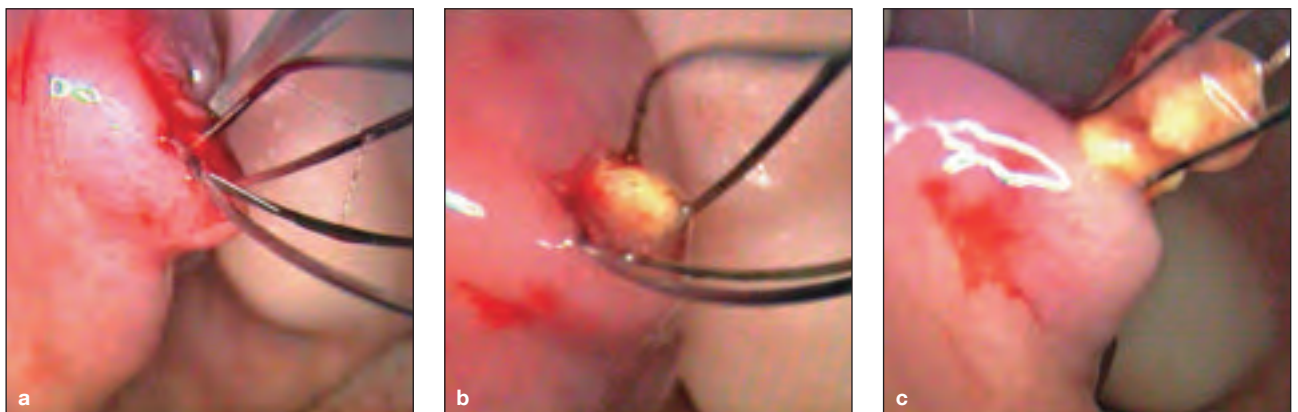
On contact with the endoscope, the stone disintegrates into fragments.



Figs. 4.26a, b
The stone fragments are progressively extracted with the basket.

Stone Extraction by Mini-Papillotomy

If the individual stones or fragments are too large for removal through the distended or dilated papilla, it may be necessary to make an incision in the papillary region (mini-papillotomy). Especially in the case of the parotid papilla, however, the papillary incision should be no longer than approximately 3–4 mm to prevent scarring and papillary stenosis.



Figs. 4.27a–c
A stone retrieved in the basket has become lodged in the papilla, requiring extraction through a mini-papillotomy. Stent insertion is unnecessary following stone removal.

4.2 Sialendoscopic Techniques in Noncalcified Obstructions

4.2.1 Acute Obstructive Sialodochitis

Acute ductal inflammation (sialodochitis), like a stenosis or stricture, has an indeterminate etiology in up to 50% of cases. Chronic recurrent parotitis appears to be a very frequent cause, however. Sonography can provide evidence of an obstruction (Fig. 4.28).

Recurrent sialodochitis may be accompanied by the formation of soft mucous plaques (Figs. 4.29) or fibrinoid plaques that have already undergone a degree of fibrous change (Fig. 4.30), leading to duct obstruction with consequent glandular swelling.

Treatment consists of repeated irrigations with a corticosteroid solution (250 milligrams of Prednisolone in 50 mL Ringer solution) and removal of the mucous or fibrinous plaques. This provides local treatment for acute inflammation and restores ductal patency.

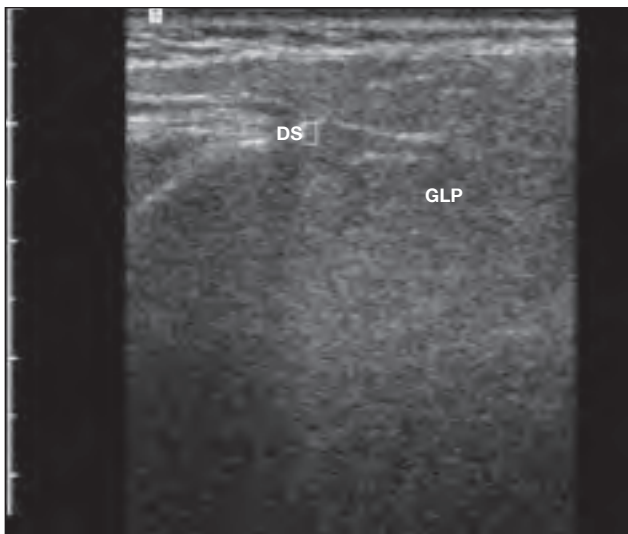
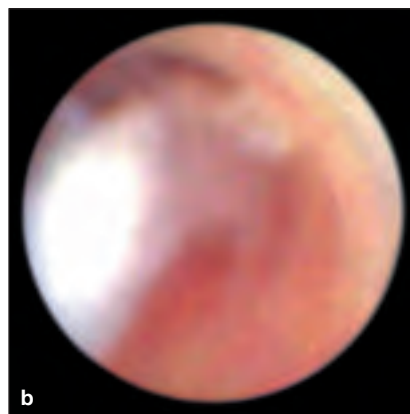


Fig. 4.28
Ultrasound appearance of acute sialodochitis. The parenchyma shows only subtle hypoechoic change and there is mild dilatation of the duct system.



Figs. 4.29a, b
Typical signs of acute sialodochitis are redness of the mucosa, edema, fibrinous exudation (a, submandibular duct), and the formation of fibrinoid mucus with a potential obstructive effect (b, submandibular duct).



Fig. 4.30
Obstructive fibrinous plaque, already partly organized, in the parotid duct.

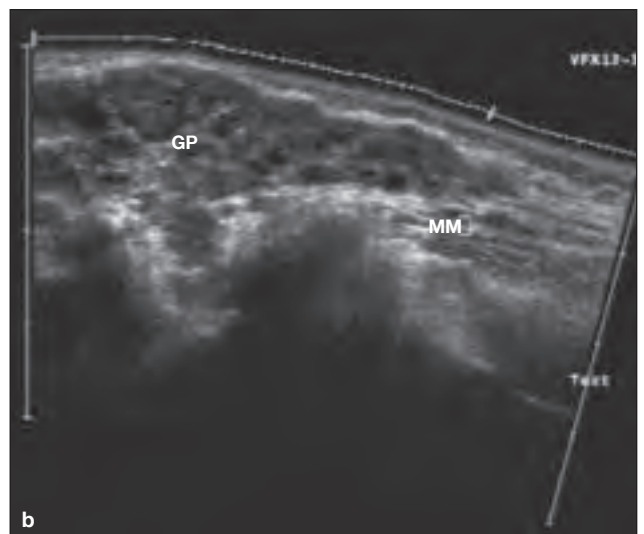
4.2.2 Chronic Recurrent Sialodochitis and Sialadenitis

Chronic obstructive changes in the ductal epithelium are found in patients with chronic recurrent (juvenile) parotitis, also after radioiodine therapy or radiotherapy and in autoimmune diseases with salivary gland involvement (e.g., Sjögren syndrome). Generally these

pathologies cannot be specifically diagnosed with ultrasound because the glandular parenchyma often shows nonspecific hypoechoic changes.

Again, sialendoscopy can at least provide insight into the nature of the ductal changes. The ductal epithe-

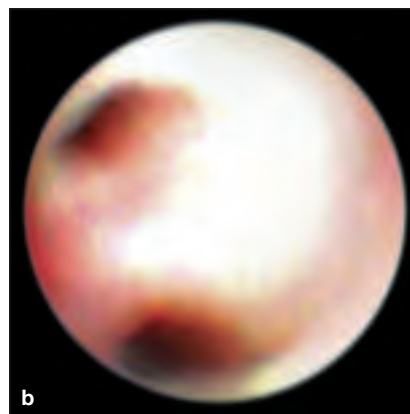
lium is whitish, thickened, and stiff with no detectable circular ridges (**Figs. 4.32a, b**). Fibrinous exudates are consistently found, and some cases show at least a propensity for stenosis.



Figs. 4.31a, b

Sonographic appearance of chronic obstructive sialodochitis with sialadenitis after radioiodine therapy. The gland is small, the glandular parenchyma is hypoechoic, and there is mild obstructive dilatation of the parotid duct. (**b**) Chronic recurrent juvenile parotitis.

The parenchyma of the parotid gland (**GP**) shows cloudy changes with multiple areas of local ductal dilatation (**MM** = masseter muscle, **GP** = parotid gland, **DS** = Stensen's duct, **UK** = mandible).



Figs. 4.32a, b

Changes in the main duct (**a**) and hilar region (**b**) following radioiodine therapy.



Fig. 4.33
A 22-gauge (0.9-mm) blunt-tipped needle is placed on a syringe with plunger for local therapy and intraductal injection of medications.

Treatment consists of irrigation with a corticosteroid drug (250 milligrams of prednisolone in 50 mL Ringer's solution) and, if necessary, removal of obstructing mucous plaques under endoscopic vision. This can prevent or at least delay persistent inflammatory ductal and glandular changes and even the development of significant stenosis. The dilatation of stenoses can also be performed (see below). Intraductal administration of a corticosteroid drug has also proven effective after interventional procedures. In the standard regimen, intraductal injections of 50 mg of prednisolone are given once a week for 6 weeks. The cortisone is injected with a blunt-tipped needle and massaged into the gland.

4.2.3 Stenoses and Strictures

Noncalcified obstructions such as stenoses and strictures are responsible for salivary gland swelling in 25% to over 50% of cases. Strictures and stenoses often develop

in a setting of chronic recurrent parotitis, but up to 50% have an unknown cause. As with other ductal lesions, ultrasound is the primary imaging procedure, providing valu-

able information on the extent and location of stenosis. Typically it shows a hypoechoic band indicating congestion of the proximal duct segments.

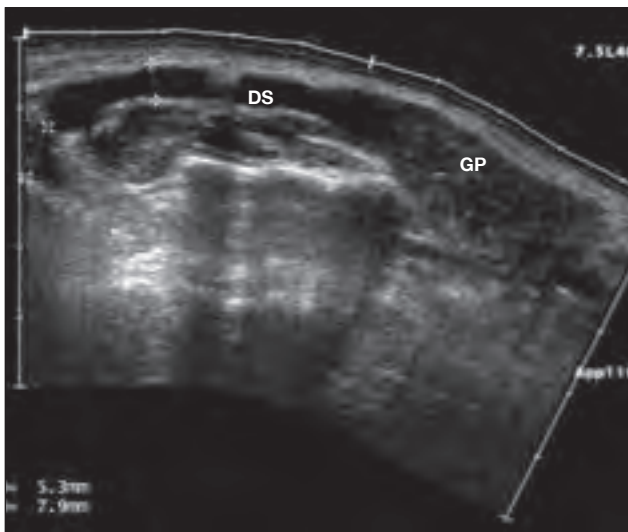


Fig. 4.34
Sonographic appearance of stenosis of the left parotid duct (**DS**). As is usually the case, the dilated proximal duct system appears as a hypoechoic band (**GP**). The parotid gland (**GP**) shows decreased echogenicity and inflammatory enlargement.



Fig. 4.35
Fibrous stricture of the submandibular duct, showing almost complete obliteration of the hilar region.

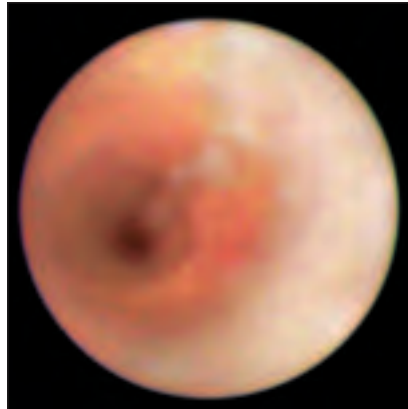


Fig. 4.36
Fibrous filiform stricture of the parotid duct.

Ultimately, sialendoscopy is the only modality that allows the composition, structure, and extent of a ductal stenosis to be accurately diagnosed and evaluated. Stenoses rarely have an acute inflammatory cause. The majority are fibrous and result from postinflammatory scarring. Fibrous strictures require

treatment by intraluminal dilatation, which is generally performed with a micro burr or wire basket and may be combined with stent insertion. A few cases are managed by balloon dilatation. This is performed with high-pressure balloons whose inflation pressure is controlled with an attached pump (Sialotechnology,

Ashkelon, Israel). The goal is to expand the duct lumen until salivary flow is restored and effective conservative therapy (sialagogues, glandular massage) can again be provided. Stent insertion is indicated in cases with a severe inflammatory reaction, long segmental lesions, or significant papillary injuries.



Figs. 4.37a, b
High-pressure balloon connected to the pump (a) and inflated (b).

Dilatation of Submandibular Duct Stricture with the Wire Basket

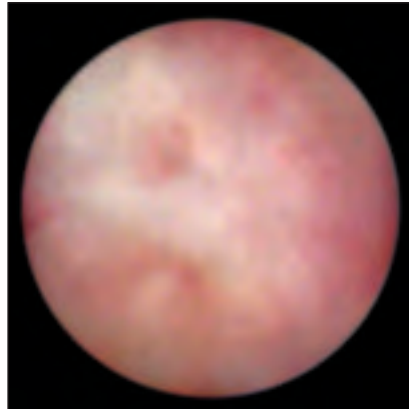


Fig. 4.38
Almost complete obliteration of the hilar region of the submandibular gland.



Fig. 4.39
First the stricture is dilated with a wire basket.

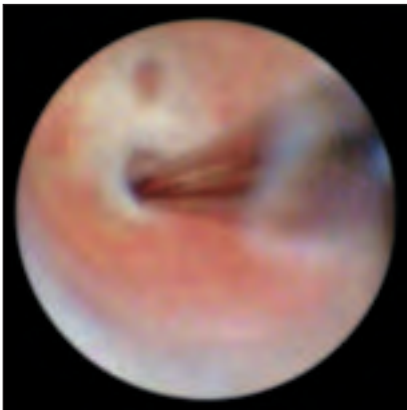
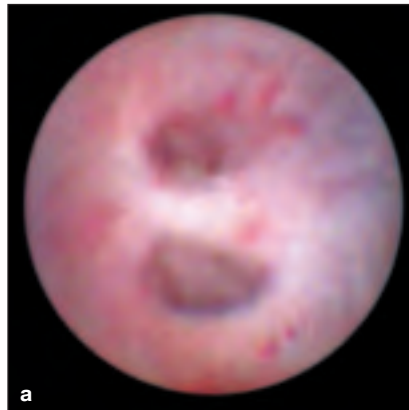
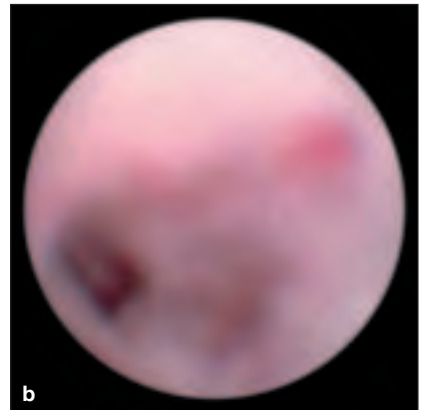


Fig. 4.40
Progressive dilatation of the main branches.



Figs. 4.41a, b
Final appearance after dilatation of the main branches (a) and view into a main branch through the dilated stricture (b).



Dilatation of Parotid Duct Stricture with the Wire Basket

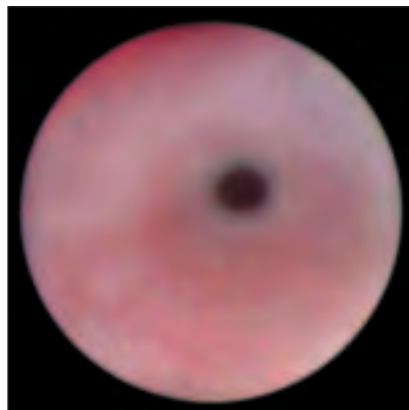


Fig. 4.42
Filiform stricture of the parotid duct.



Fig. 4.43
Dilatation of the stricture with the wire basket.



Fig. 4.44
Appearance following dilatation.

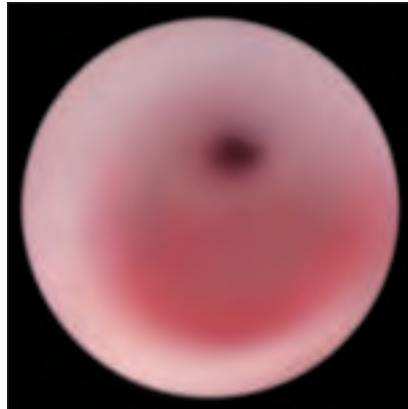


Fig. 4.45
View of the hilar region through the dilated stricture.

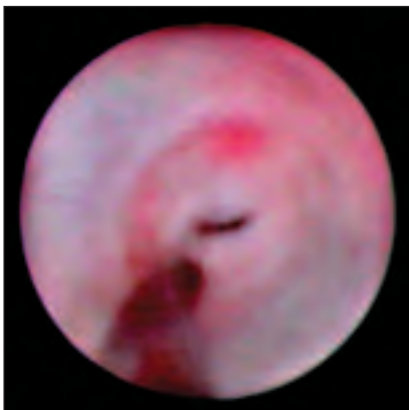


Fig. 4.46
Almost complete obliteration of the hilar region of the parotid gland and initial dilatation with a micro burr.

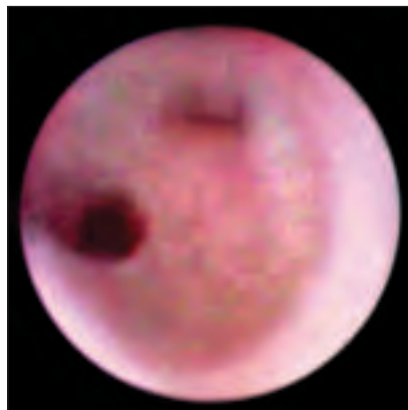


Fig. 4.47
Progressive dilatation of the main branches.

Treatment of Parotid Duct Stenosis by Dilatation with a Micro Burr

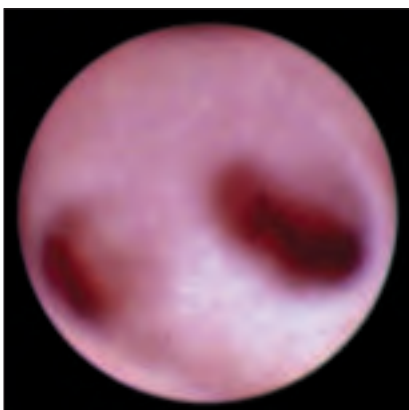


Fig. 4.48
View after dilatation of the main branches.

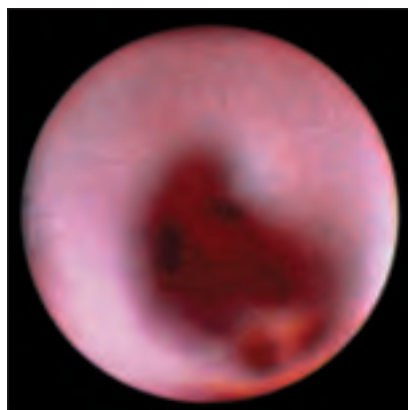


Fig. 4.49
View into one of the main branches after dilatation. The prestenotic duct structure and additional branches can be seen.

The procedure concludes with cortisone irrigation (250 mg of prednisolone in 50 mL Ringer's solution) under endoscopic control. The postintervention regimen consists of intraductal cortisone injections of 50 mg of prednisolone given once a week for 6 weeks. In most cases this can prevent the recurrence or progression of stenosis.



Fig. 4.50
Stents (Sialotechnology, Ashkelon, Israel). These are very flexible, biocompatible Teflon stents with soft barbs or basket-like expanders to prevent migration. The stents are available in various lengths (20–40 mm) and widths (3–6 F).



Fig. 4.51
The stent is fitted over the endoscope in preparation for endoscopically controlled insertion.

Endoscopically Controlled Stent Insertion

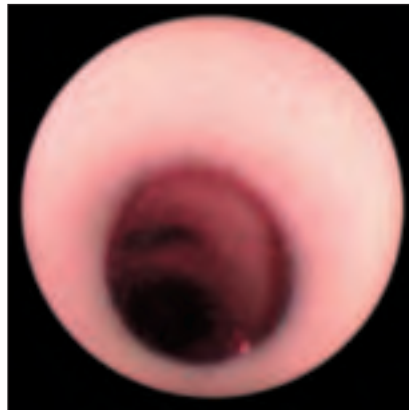


Fig. 4.52
Stent in situ following endoscopically controlled insertion. The more proximal duct system with its branches is visible through the stent.



Fig. 4.53
Stent in situ and secured to the buccal mucosa with sutures (2–4 interrupted Vicryl sutures). The stent should remain in place for approximately 6–8 weeks to prevent restenosis.

4.2.4 Foreign Bodies

Intraductal foreign bodies consist mainly of natural fibers (grass, hay particles, facial hairs) or plastics (e.g., pieces of toothbrush bristles). Most foreign bodies are echogenic enough to be detected sonographically but cannot be positively identified.

Sialendoscopy is the only procedure that can accurately characterize foreign bodies, determine their location, and retrieve them if necessary.

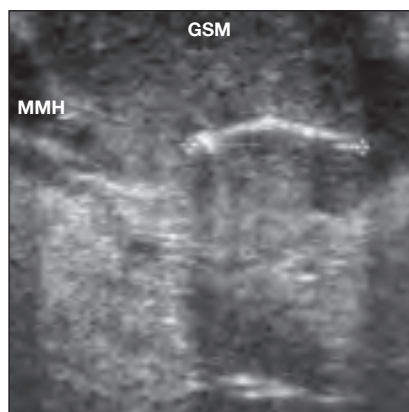


Fig. 4.54
Sonographic appearance of a foreign body in the submandibular gland (**GSM**). The object appears as an intraparenchymal hyperechogenic structure without an acoustic shadow. It was identified postoperatively as a plant fiber.

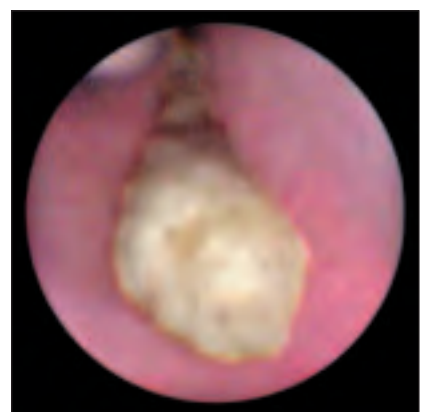


Fig. 4.55
Superficial mineral deposits have formed on this intraductal hair, causing obstruction of the submandibular duct. The hair was removed with a wire basket.



Fig. 4.56
Endoscopic detection of two intraductal wire remnants following the attempted basket extraction of a stone.

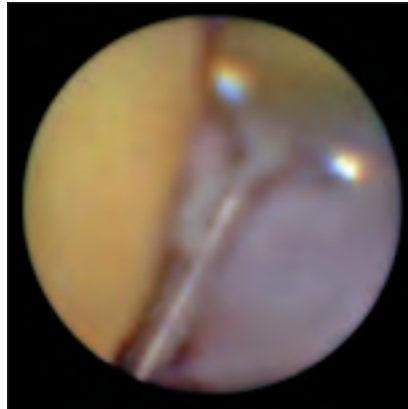


Fig. 4.57
One of the wires is grasped with the forceps.

Foreign Body Removal (Basket Remnant) with the Endoscopic Forceps

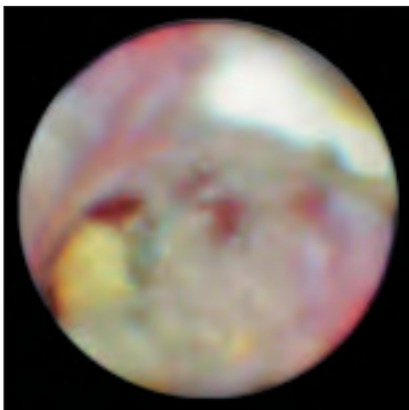


Fig. 4.58
A wire is mobilized and extracted with the forceps. The wires were lodged in the stone and also in the duct wall.

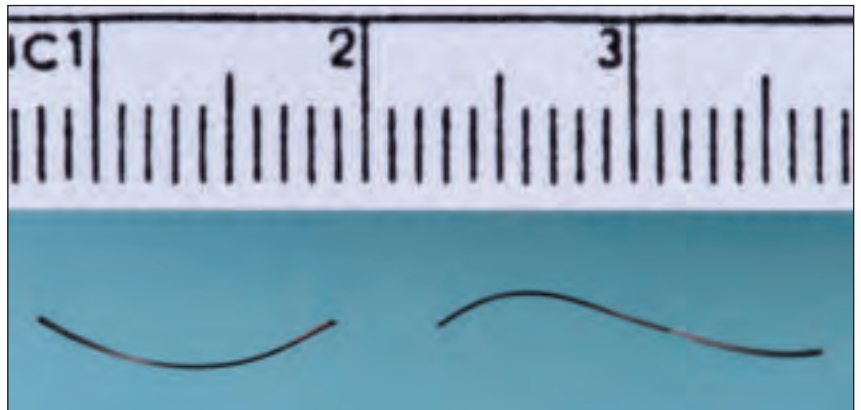


Fig. 4.59
Wire fragments broken from a retrieval basket.

4.3 Follow-up Care

It is important to ensure adequate salivary flow after sialendoscopy. Salivation is most effectively stimulated by administering natural stimulants and by manual manipulation (glandular massage). Interventional procedures, especially when prolonged and associated with trauma to the duct walls, require antibiotic prophylaxis along with measures to reduce swelling.

4.4 Morbidity and Complications

Slight swelling of the salivary glands is consistently present for 2–3 hours after sialendoscopy as a result of the irrigation. Complications such as hematoma formation, duct perforation,

duct strictures, ranula formation, and nerve lesions (lingual nerve, facial nerve) are very rare when proper technique is used.

4.5 Indications and Contraindications to Sialendoscopy

The possible applications of sialendoscopy have expanded markedly in recent years as a result of technical advances.

Indications:

Diagnosis and Treatment of Sialolithiasis

Sialendoscopy can contribute significantly to the detection of occult stones. It also permits the diagnosis of mucous and fibrinous plaques, thus making an important contribution to detecting the early stages of stone formation. It is conceivable

that stone formation could be prevented by plaque removal and irrigation. In many cases, endoscopy is the only modality that can determine whether stones can be managed best by interventional therapy, transoral duct incision,

ESWL, or a combination of treatments. Sialendoscopy also permits the follow-up or completion of a previous therapeutic procedure such as residual stone removal after ESWL.

Diagnosis and Treatment of Noncalcified Obstructions

Sialendoscopy is of substantial value in the diagnosis and treatment of stenoses, strictures, foreign bodies, and intraductal masses. Stenoses and strictures can be dilated with the instruments available, and foreign bodies can be removed. Through direct visualiza-

tion of the affected region, sialendoscopy can identify other causes of salivary gland swelling such as anatomic variants and malformations, which are poorly accessible to indirect imaging studies. Sialendoscopy can also give new insights into the pathology of specific salivary

gland diseases such as recurrent juvenile parotitis, and it provides new opportunities to assess the concomitant or secondary involvement of the salivary glands in other disorders such as autoimmune diseases.

Assessment of Treatment Outcomes

The normalization of glandular function after the elimination of pathology can not only be confirmed clinically but can also be assessed

by follow-up sialendoscopy based on the regression of wall thickness and inflammatory signs.

Contraindications

Today the only contraindication to sialendoscopy is an acute, suppurative inflammation of the salivary gland.

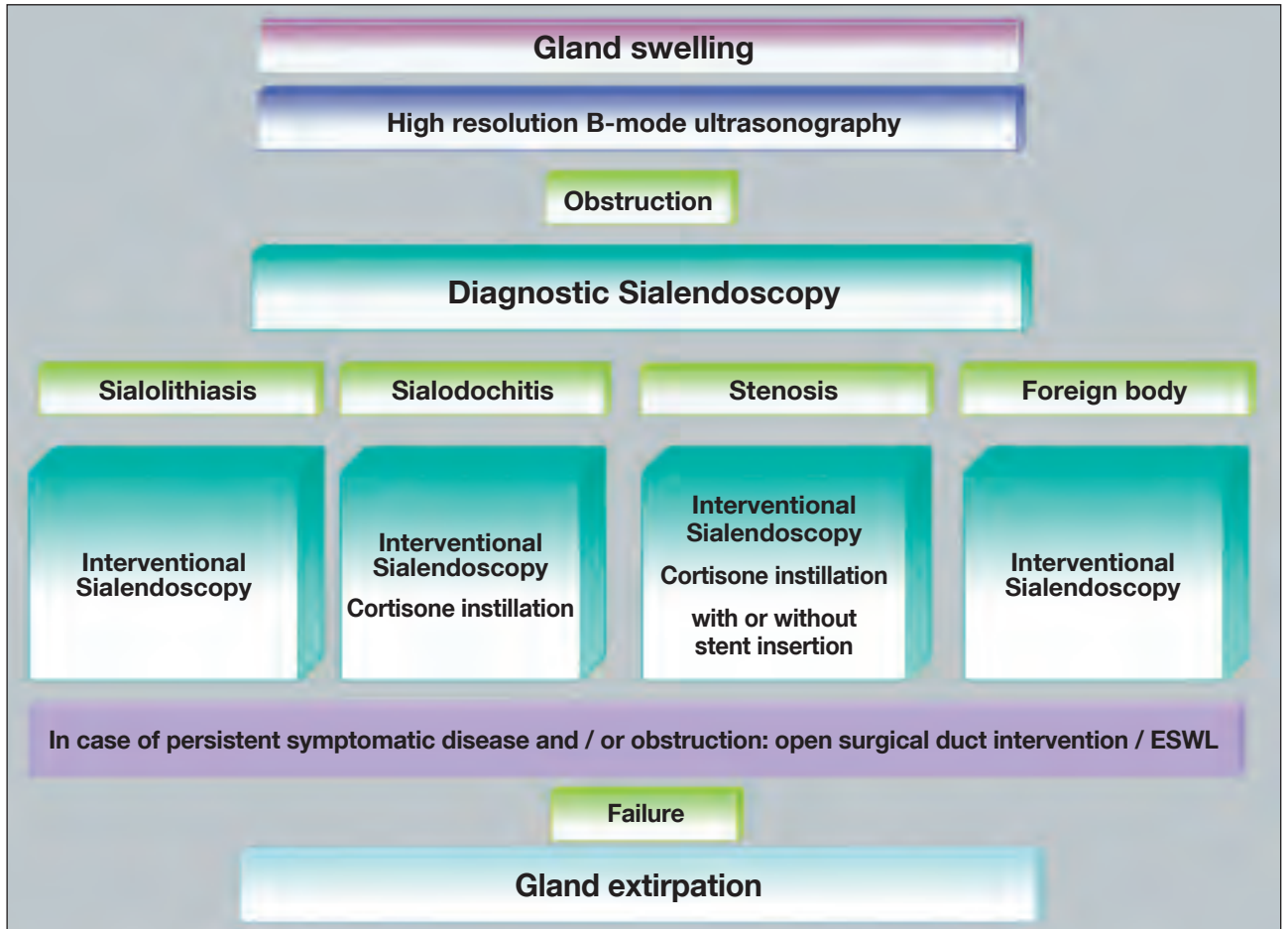


Fig. 4.60
Flowchart for the diagnosis and treatment of obstructive diseases of the major salivary glands.

5.0 Summary

In recent years the optimization of endoscopes in terms of image quality, dimensions, and ease of use has led to their safe and effective use in obstructive diseases of the major salivary glands. Salivary

duct endoscopy can detect pathologies that have previously been undetectable even by sophisticated imaging procedures. Concurrent with these advances in diagnosis, new endoscopically assisted thera-

peutic procedures have also been established. These procedures have helped make it possible to preserve the affected gland in the great majority of cases.

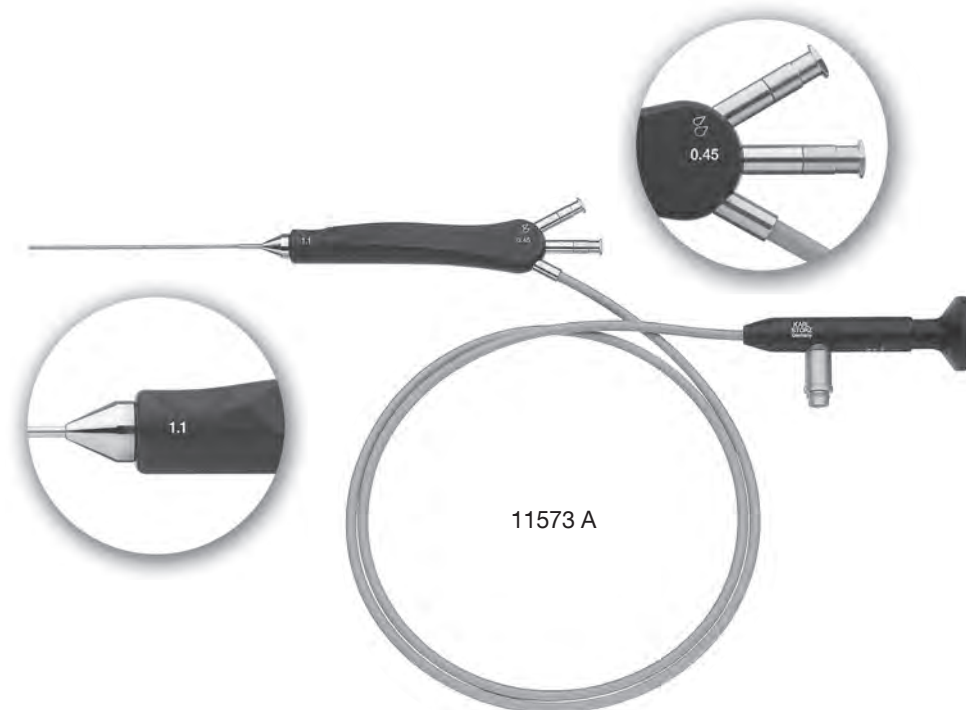
6.0 References

1. ARZOZ E, SANTIAGO A, ESNAL F, PALOMERO R (1996): Endoscopic intracorporeal lithotripsy for sialolithiasis. *J Oral Maxillofac Surg* 54: 847–50
2. AVRAHAMI E, ENGLENDER M, CHEN E, SHABTAY D, KATZ R, HARELL M (1996): CT of submandibular gland sialolithiasis. *Neuroradiology* 38: 287–90
3. CHU D W, CHOW T L, LIM B H, KWOK S P (2003): Endoscopic management of submandibular sialolithiasis *Surg Endosc* 17(6): 876–9
4. DRAGE NA, WILSON RF, MCGURK M: The genu of the submandibular duct – is the angle significant in salivary gland disease? *Dentomaxillofac Radiol.* 2002 Jan;31(1):15–8
5. FÖDRA C, KAARMANN H, IRO H (1992): Sonographie und Röntgennativaufnahme in der Speichelsteindiagnostik – experimentelle Untersuchungen. *HNO* 40: 25–28
6. GRITZMANN N, HAJEK P (1985): Sonographie bei Speichelsteinen – Indikationen und Stellenwert. *ROFO Fortschr Geb Röntgenstr Nuklearmed* 1985; 142: 559–62
7. GUNDLACH P, HOPF J, LINNARZ M (1994): Introduction of a new diagnostic procedure: salivary duct endoscopy (sialendoscopy). Clinical evaluation of sialendoscopy, sialography, and x-ray imaging. *End Surg Allied Technol* 2: 294–6
8. IRO H, ZENK J, WALDFAHRER F, BENZEL W, SCHNEIDER T, ELL C (1998): Extracorporeal shock wave lithotripsy of parotid stones. Results of a prospective clinical trial. *Ann Otol Rhinol Laryngol.* Oct;107(10 Pt 1):860–4.
9. IRO H, SCHNEIDER HT, FÖDRA C, WAITZ G, NITSCHKE N, HEINRITZ HH, BENNINGER J, ELL C (1992): Shockwave lithotripsy of salivary duct stones. *Lancet.* May 30;339(8805):1333–6
10. IRO H, WAITZ G, NITSCHKE N, BENNINGER J, SCHNEIDER T, ELL C. (1992): Extracorporeal piezoelectric shock-wave lithotripsy of salivary gland stones. *Laryngoscope.* May;102(5):492–4
11. IRO H, ZENK J, BENZEL W (1995): Laser lithotripsy of salivary duct stones. *Adv Otorhinolaryngol* 1995; 49:148–52
12. IRO H, ZENK J, WALDFAHRER F, BENZEL W (1996): Aktueller Stand der minimal invasiven Behandlungsverfahren bei der Sialolithiasis. *HNO* 44: 78–84
13. IRO H, ZENK J (2003): Konzepte zur Diagnostik und Therapie des Speichelsteinleidens. *Deutsches Ärzteblatt* 100 (9): 556–62
14. ISACSSON G, ISBERG A, HAVERLING M, LUNDQUIST PG (1984): Salivary calculi and chronic sialoadenitis of the submandibular gland: a radiographic and histologic study. *Oral Surg Oral Med Oral Pathol.* 1984 Nov;58(5):622–7
15. KALINOWSKI M, HEVERHAGEN JT, REHBERG E, KLOSE KJ, WAGNER HJ (2002): Comparative study of MR sialography and digital subtraction sialography for benign salivary gland disorders. *AJNR Am J Neuroradiol* 23(9): 1485–92
16. KATZ P (1991): Endoscopie des glandes salivaires. *Ann Radiol* 34: 110–13
17. KATZ P, FRITSCH M H (2003): Salivary stones: innovative techniques in diagnosis and treatment. *Curr Opin Otolaryngol Head Neck Surg* 11(3): 173–8
18. KATZ P. (2004): New techniques for the treatment of salivary lithiasis: sialoendoscopy and extracorporeal lithotripsy: 1773 cases. *Ann Otolaryngol Chir Cervicofac.* 2004 Jun;121(3):123–32
19. KOCH M, ZENK J, BOZZATO A, BUMM K, IRO H. (2005): Sialoscopy in cases of unclear swelling of the major salivary glands. *Otolaryngol Head Neck Surg.* 2005 Dec;133(6):863–8
20. KOCH M, ZENK J, IRO H: Die Speichelgangendoskopie in der Diagnostik und Therapie von obstruktiven Speicheldrüsen-Erkrankungen. *HNO* (accepted for publication)
21. KÖNIGSBERGER R, FEYH J, GOETZ A, SCHILLING V, KASTENBAUER E (1990): Endoscopically controlled laser lithotripsy in the treatment of sialolithiasis. *Laryngorhinootologie* 69(6): 322–3

22. MARCHAL F, BECKER M, VAVRINA J, DULGEROV P, LEHMANN W (1997): Diagnostic traitement de sialolithiasis. *Bull med suisses* 79;1023–027
23. MARCHAL F, BECKER M, DULGUEROV P, LEHMANN W (2000): Interventional sialendoscopy. *Laryngoscope* 110 (2Pt1): 318–20
24. MARCHAL F, BECKER M, DULGUEROV P, LEHMANN W (2001): Specificity of parotid sialendoscopy. *Laryngoscope* 111: 264–71
25. MARCHAL F, DULGUEROV P, BECKER M, BARKI G, FRANCOIS D, LEHMANN W (2002): Submandibular diagnostic and interventional sialendoscopy: new procedure for ductal disorders. *Ann Otol Rhinol Laryngol* 111: 27–35
26. MCGURK M, ESCUDIER M P, THOMAS B L, BROWN J E (2006): A revolution in the management of obstructive salivary gland disease. *Dent Update* 33(1): 28–30, 33–6
27. NAHLIELI O, BARUCHIN AM (1999): Endoscopic technique for the diagnosis and treatment of obstructive salivary gland diseases. *J Oral Maxillofac Surg* 57: 1394–1401
28. NAHLIELI O, NEDER A, BARUCHIN AM (1999): Salivary gland endoscopy: a new technique for the diagnosis and treatment of sialolithiasis. *J Oral Maxillofac Surg* 52: 1240–42
29. NAHLIELI O, BARUCHIN AM (2000): Long-term experience with endoscopic diagnosis and treatment of salivary gland inflammatory diseases. *Laryngoscope* 110 (6): 988–93
30. NAHLIELI O, SHACHAM R, YOFFE B, ELIAV E: Diagnosis and treatment of strictures and kinks in salivary gland ducts. *J Oral Maxillofac Surg*. 2001 May;59(5):484–90; discussion, 490–2
31. NAHLIELI O, SHACHAM R, SHLESINGER M, ELIAV E (2004): Juvenile recurrent parotitis: a new method of diagnosis and treatment. *Pediatrics* 114(1): 9–12
32. NAHLIELI O, NAKAR LH, NAZARIAN Y, TURNER MD: Sialoendoscopy: A new approach to salivary gland obstructive pathology. *J Am Dent Assoc*. 2006 Oct;137(10):1394–400. Review
33. NAKAYAMA E, YUASA K, BEPPU M, KAWAZU T, OKAMURA K, KANDA S (2003): Interventional sialendoscopy: a new procedure for noninvasive insertion and a minimally invasive sialolithectomy. *J Oral Maxillofac Surg* 61(10): 1233–6
34. NGU RK, BROWN JE, WHAITES EJ, DRAGE NA, NG SY, MAKDISSI J: Salivary duct strictures: nature and incidence in benign salivary obstruction. *Dentomaxillofac Radiol*. 2007 Feb;36(2):63–7
35. QI S, LIU X, WANG S (2005): Sialoendoscopic and irrigation findings in chronic obstructive parotitis. *Laryngoscope* 115(3): 541–5
36. RICE DH: Non-inflammatory, non-neoplastic disorders of the salivary glands (1999) *Otolaryngol Clin North Am* 32: 835–43
37. RICE DH: Chronic inflammatory disorders of the salivary glands (1999) *Otolaryngol Clin North Am* 32:813–18
38. VARGHESE JC, THORNTON F, LUCEY BC, WALSH M, FARRELL MA, LEE MJ (1999): A prospective comparative study of MR sialography and conventional sialography of salivary gland disease. *AJR Am Roentgenol* 173(6): 1497–503
39. YUASA K, NAKHYAMA E, BAN S, KAWAZU T, CHIKUI T, SHIMIZU M, KANDA S (1997): Submandibular gland duct endoscopy. Diagnostic value for salivary duct disorders in comparison to conventional radiography, sialography, and ultrasonography. *Oral Surg Oral Med Oral Pathol Oral Radiol Endo* 84: 578–81
40. ZENK J, IRO H (2001): Die Sialolithiasis und deren Behandlung. *Laryngo-Rhino-Otol* 80 (Suppl): 115–136
41. ZENK J, HOSEMANN WG, IRO H: Diameters of the main excretory ducts of the adult human submandibular and parotid gland: a histologic study. *Oral Surg Oral Med Oral Pathol Oral Radiol Endod*. 1998 May;85(5):576–80
42. ZENK J, KOCH M, BOZZATO A, IRO H (2004): Sialoscopy – initial experiences with a new endoscope. *Br J Oral Maxillofac Surg* 42(4): 293–8
43. ZIEGLER C M, STEVELING H, SEUBERT M, MUHLING J (2004): Endoscopy: a minimally invasive procedure for diagnosis and treatment of diseases of the salivary glands. Six years of practical experience. *Br J Oral Maxillofac Surg*; 42(1): 1–7

ERLANGEN Miniature Endoscopes

For the diagnosis and treatment of obstructive salivary gland diseases



- 11572 A **Miniature Straight Forward Telescope 0°**,
O.D. 0.8 mm, NiTi, semiflexible, with scale, **autoclavable**,
irrigation channel I.D. 0.25 mm, working length 10 cm,
length 140 cm remote eyepiece,
fiber optic light transmission incorporated
- 11573 A **Miniature Straight Forward Telescope 0°**,
O.D. 1.1 mm, NiTi, semiflexible, with scale, **autoclavable**,
working channel I.D. 0.45 mm, irrigation channel I.D. 0.25 mm,
working length 10 cm, length 140 cm remote eyepiece,
fiber optic light transmission incorporated,
for use with:
– **Stone Extractor** 11582 M/11573 NP/11573 M
– **Micro Burr** 11573 MB
– **Guide Wire** 745725
– **Laser Probe**
- 11574 A **Miniature Straight Forward Telescope 0°**,
O.D. 1.6 mm, NiTi, semiflexible, with scale, **autoclavable**,
working channel I.D. 0.85 mm, irrigation channel I.D. 0.25 mm,
working length 10 cm, length 140 cm remote eyepiece,
fiber optic light transmission incorporated,
– **Stone Extractor** 11582 M/11573 NP/11573 M
– **Micro Burr** 11574 MB
– **Foreign Body Forceps** 11574 TJ
– **Biopsy Forceps** 11574 ZJ
– **Guide Wire** 745720
– **Laser Probe**
– **Balloon Catheter** 11583 BP

It is recommended to check the suitability of the product for the intended procedure prior to use.

ERLANGEN Miniature Endoscopes

For the diagnosis and treatment of obstructive salivary gland diseases

Grasping Forceps



11574 TJ



11574 TJ

Foreign Body Forceps, flexible, double action jaws, diameter 0.8 mm, working length 30 cm, for use with Miniature Straight Forward Telescopes 11574 A and 11583 A



11574 ZJ

Biopsy Forceps, flexible, double action jaws, diameter 0.8 mm, working length 30 cm, for use with Miniature Straight Forward Telescopes 11574 A and 11583 A

Stone Extractor and Micro Burr



11582 M

Stone Extractor, diameter 0.4 mm, basket with 4 wires, sterile, for single use



11573 NP

Front-loading Stone Extractor, without handle, diameter 0.4 mm, length 35 cm, basket with 4 wires, sterile, for single use, package of 10



11573 M

Stone Extractor, diameter 0.4 mm, basket with 4 wires, handle for fixation to endoscope



11573 MB

Micro Burr for Salivary Stones, diameter 0.38 mm, for use with Miniature Straight Forward Telescopes 11573 A and 11582 A

11574 MB

Same, diameter 0.8 mm, for use with Telescopes 11574 A and 11583 A

Balloon Catheter



11583 BP

Balloon Catheter, diameter 0.7 mm, sterile, for single use, package of 10, for use with Telescopes 11574 A and 11583 A

Dilator



745910



745910

Dilator, for Salivary Duct, length 14 cm



745920



745920

Dilator, for Salivary Duct, size 1, diameter 0.5 – 0.8 mm, length 11.5 cm

745921

Same, size 2 diameter 0.7–1.0 mm, length 11.5 cm

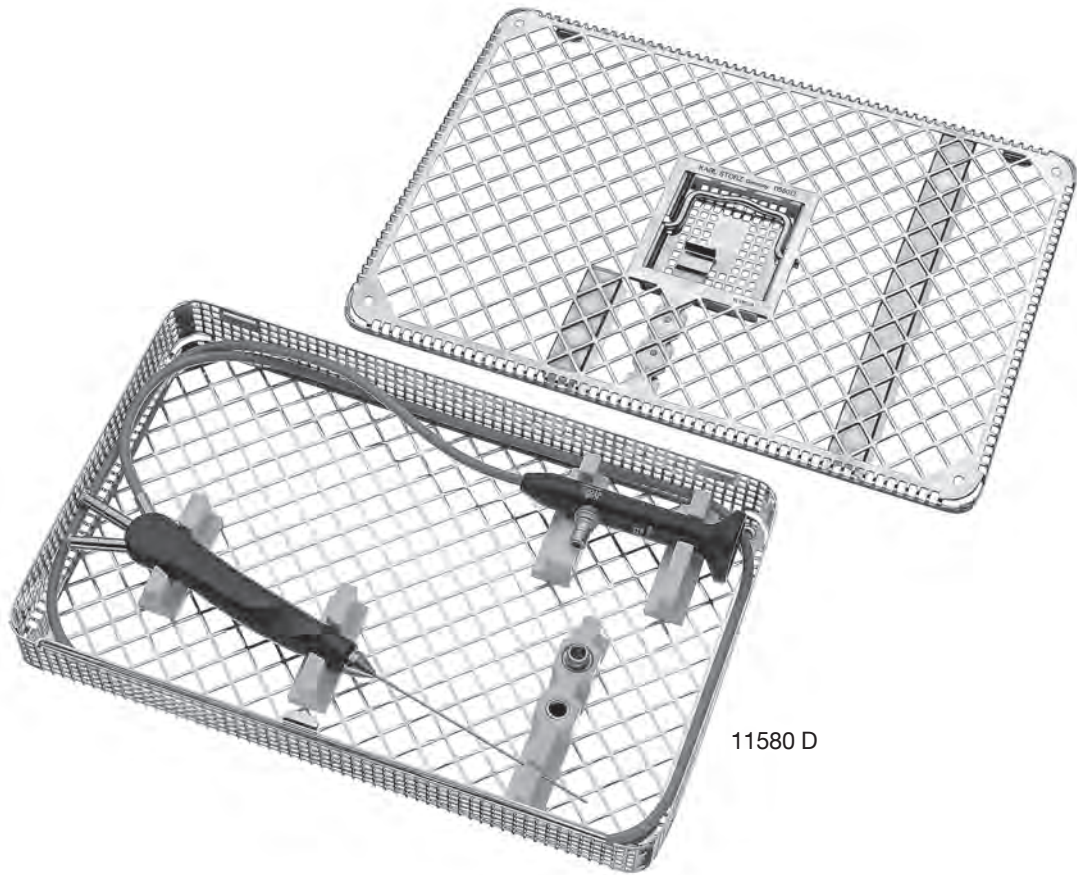
745922

Same, size 3 diameter 0.9–1.2 mm, length 11.5 cm

745923

Same, size 4 diameter 1.0–1.1 mm, length 11.5 cm

Metal Tray for Sterilization and Storage



11580 D

11580 D **Metal Tray**, for Sterilization and Storage of a Miniature Straight Forward Telescope 11572 A – 11574 A, perforated, lid with silicone bridges, external dimensions (w x d x h): 275 x 175 x 37 mm

Cleaning

27651 K1 **Cleaning Brush** for working channel diameter 0.4 – 0.6 mm, length 40 cm, for single use, package of 10
 27651 K2 **Same**, for working channel diameter 0.6 – 0.8 mm
 27651 K3 **Same**, for working channel diameter 0.8 – 1.4 mm
 27651 K5 **Same**, for working channel diameter 0.25 – 0.4 mm

IMAGE1 S Camera System ^{NEW}



Economical and future-proof

- Modular concept for flexible, rigid and 3D endoscopy as well as new technologies
- Forward and backward compatibility with video endoscopes and FULL HD camera heads



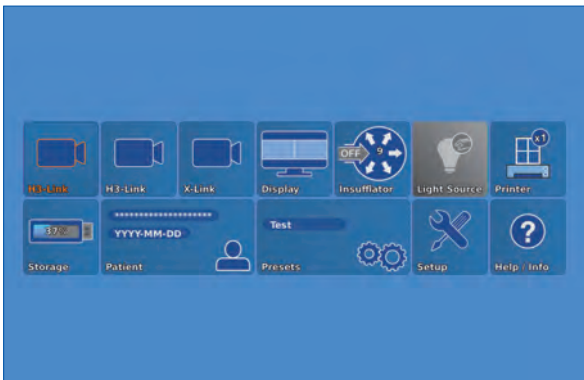
- Sustainable investment
- Compatible with all light sources



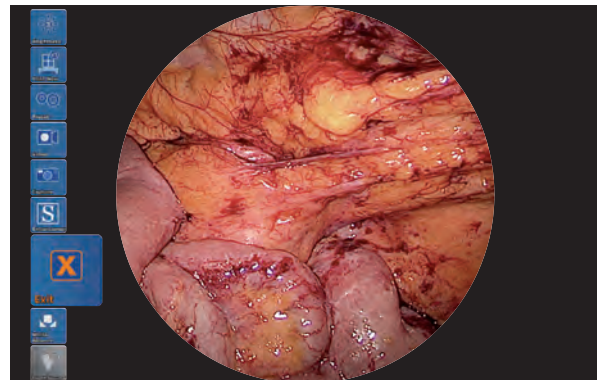
Innovative Design

- Dashboard: Complete overview with intuitive menu guidance
- Live menu: User-friendly and customizable
- Intelligent icons: Graphic representation changes when settings of connected devices or the entire system are adjusted

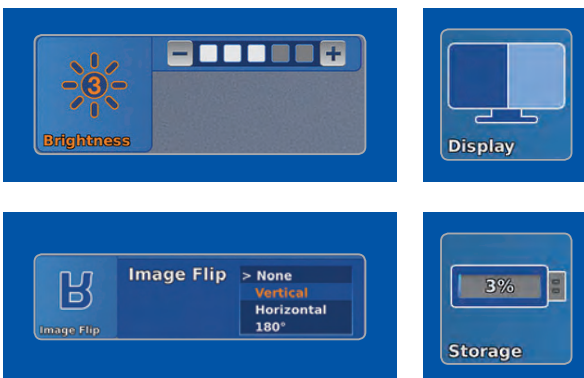
- Automatic light source control
- Side-by-side view: Parallel display of standard image and the Visualization mode
- Multiple source control: IMAGE1 S allows the simultaneous display, processing and documentation of image information from two connected image sources, e.g., for hybrid operations



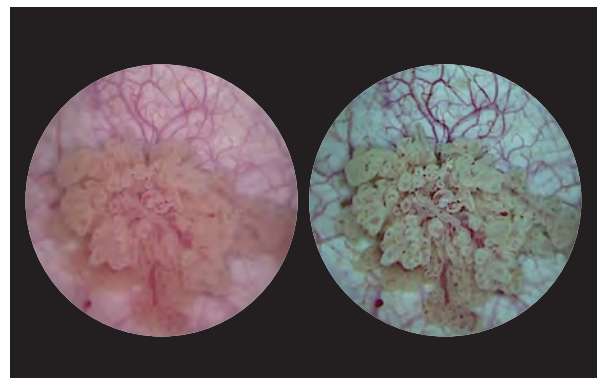
Dashboard



Live menu



Intelligent icons



Side-by-side view: Parallel display of standard image and Visualization mode

IMAGE1 S Camera System ^{NEW}

IMAGE1 S

Brilliant Imaging

- Clear and razor-sharp endoscopic images in FULL HD
- Natural color rendition

- Reflection is minimized
- Multiple IMAGE1 S technologies for homogeneous illumination, contrast enhancement and color shifting



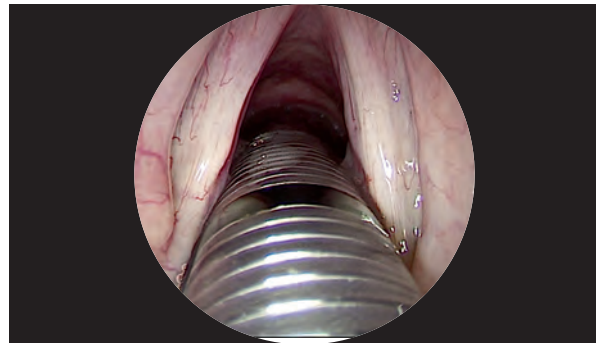
FULL HD image



CLARA



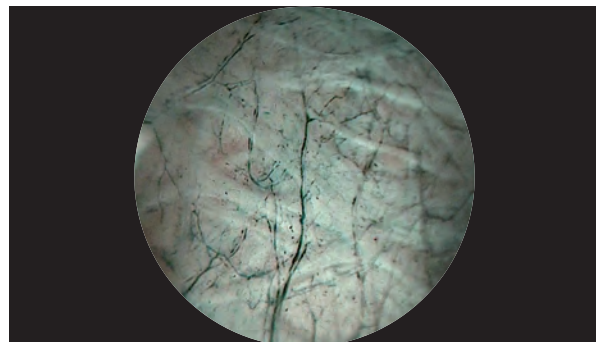
FULL HD image



CHROMA



FULL HD image



SPECTRA A*



FULL HD image



SPECTRA B**

* SPECTRA A: Not for sale in the U.S.

** SPECTRA B: Not for sale in the U.S.

IMAGE1 S Camera System ^{NEW}



TC 200EN

TC 200EN* **IMAGE1 S CONNECT**, connect module, for use with up to 3 link modules, resolution 1920 x 1080 pixels, with integrated KARL STORZ-SCB and digital Image Processing Module, power supply 100–120 VAC/200–240 VAC, 50/60 Hz including:
Mains Cord, length 300 cm
DVI-D Connecting Cable, length 300 cm
SCB Connecting Cable, length 100 cm
USB Flash Drive, 32 GB, USB silicone keyboard, with touchpad, US
*** Available in the following languages:** DE, ES, FR, IT, PT, RU

Specifications:

HD video outputs	- 2x DVI-D - 1x 3G-SDI
Format signal outputs	1920 x 1080p, 50/60 Hz
LINK video inputs	3x
USB interface	4x USB, (2x front, 2x rear)
SCB interface	2x 6-pin mini-DIN

Power supply	100–120 VAC/200–240 VAC
Power frequency	50/60 Hz
Protection class	I, CF-Defib
Dimensions w x h x d	305 x 54 x 320 mm
Weight	2.1 kg

**For use with IMAGE1 S
IMAGE1 S CONNECT Module TC 200EN**



TC 300

TC 300 **IMAGE1 S H3-LINK**, link module, for use with IMAGE1 FULL HD three-chip camera heads, power supply 100–120 VAC/200–240 VAC, 50/60 Hz, **for use with IMAGE1 S CONNECT TC 200EN** including:
Mains Cord, length 300 cm
Link Cable, length 20 cm

Specifications:

Camera System	TC 300 (H3-Link)
Supported camera heads/video endoscopes	TH 100, TH 101, TH 102, TH 103, TH 104, TH 106 (fully compatible with IMAGE1 S) 22220055-3, 22220056-3, 22220053-3, 22220060-3, 22220061-3, 22220054-3, 22220085-3 (compatible without IMAGE1 S technologies CLARA, CHROMA, SPECTRA*)
LINK video outputs	1x
Power supply	100–120 VAC/200–240 VAC
Power frequency	50/60 Hz
Protection class	I, CF-Defib
Dimensions w x h x d	305 x 54 x 320 mm
Weight	1.86 kg

* SPECTRA A: Not for sale in the U.S.
 ** SPECTRA B: Not for sale in the U.S.

IMAGE1 S Camera Heads ^{NEW}

IMAGE1 S

For use with IMAGE1 S Camera System

IMAGE1 S CONNECT Module TC 200EN, IMAGE1 S H3-LINK Module TC 300
and with all IMAGE1 HUB™ HD Camera Control Units



TH 100

TH 100

IMAGE1 S H3-Z Three-Chip FULL HD Camera Head,
50/60 Hz, IMAGE1 S compatible, progressive scan,
soakable, gas- and plasma-sterilizable, with integrated
Parfocal Zoom Lens, focal length $f = 15-31$ mm (2x),
2 freely programmable camera head buttons,
for use with IMAGE1 S and IMAGE1 HUB™ HD/HD

Specifications:

IMAGE1 FULL HD Camera Heads	IMAGE1 S H3-Z
Product no.	TH 100
Image sensor	3x 1/3" CCD chip
Dimensions w x h x d	39 x 49 x 114 mm
Weight	270 g
Optical interface	integrated Parfocal Zoom Lens, $f = 15-31$ mm (2x)
Min. sensitivity	F 1.4/1.17 Lux
Grip mechanism	standard eyepiece adaptor
Cable	non-detachable
Cable length	300 cm



TH 104

TH 104

IMAGE1 S H3-ZA Three-Chip FULL HD Camera Head,
50/60 Hz, IMAGE1 S compatible, **autoclavable**,
progressive scan, soakable, gas- and plasma-sterilizable,
with integrated Parfocal Zoom Lens, focal length
 $f = 15-31$ mm (2x), 2 freely programmable camera head
buttons, for use with IMAGE1 S and IMAGE1 HUB™ HD/HD

Specifications:

IMAGE1 FULL HD Camera Heads	IMAGE1 S H3-ZA
Product no.	TH 104
Image sensor	3x 1/3" CCD chip
Dimensions w x h x d	39 x 49 x 100 mm
Weight	299 g
Optical interface	integrated Parfocal Zoom Lens, $f = 15-31$ mm (2x)
Min. sensitivity	F 1.4/1.17 Lux
Grip mechanism	standard eyepiece adaptor
Cable	non-detachable
Cable length	300 cm

Monitors



9619 NB

9619 NB

19" HD Monitor,
color systems **PAL/NTSC**, max. screen
resolution 1280 x 1024, image format 4:3,
power supply 100–240 VAC, 50/60 Hz,
wall-mounted with VESA 100 adaption,
including:
External 24 VDC Power Supply
Mains Cord



9826 NB

9826 NB

26" FULL HD Monitor,
wall-mounted with VESA 100 adaption,
color systems **PAL/NTSC**,
max. screen resolution 1920 x 1080,
image format 16:9,
power supply 100–240 VAC, 50/60 Hz
including:
External 24 VDC Power Supply
Mains Cord

Monitors

KARL STORZ HD and FULL HD Monitors	19"	26"
Wall-mounted with VESA 100 adaption	9619 NB	9826 NB
Inputs:		
DVI-D	●	●
Fibre Optic	–	–
3G-SDI	–	●
RGBS (VGA)	●	●
S-Video	●	●
Composite/FBAS	●	●
Outputs:		
DVI-D	●	●
S-Video	●	–
Composite/FBAS	●	●
RGBS (VGA)	●	–
3G-SDI	–	●
Signal Format Display:		
4:3	●	●
5:4	●	●
16:9	●	●
Picture-in-Picture	●	●
PAL/NTSC compatible	●	●

Optional accessories:

9826 SF **Pedestal**, for monitor 9826 NB

9626 SF **Pedestal**, for monitor 9619 NB

Specifications:

KARL STORZ HD and FULL HD Monitors	19"	26"
Desktop with pedestal	optional	optional
Product no.	9619 NB	9826 NB
Brightness	200 cd/m ² (typ)	500 cd/m ² (typ)
Max. viewing angle	178° vertical	178° vertical
Pixel distance	0.29 mm	0.3 mm
Reaction time	5 ms	8 ms
Contrast ratio	700:1	1400:1
Mount	100 mm VESA	100 mm VESA
Weight	7.6 kg	7.7 kg
Rated power	28 W	72 W
Operating conditions	0–40°C	5–35°C
Storage	-20–60°C	-20–60°C
Rel. humidity	max. 85%	max. 85%
Dimensions w x h x d	469.5 x 416 x 75.5 mm	643 x 396 x 87 mm
Power supply	100–240 VAC	100–240 VAC
Certified to	EN 60601-1, protection class IPX0	EN 60601-1, UL 60601-1, MDD93/42/EEC, protection class IPX2

Cold Light Fountains and Accessories



495 NL

Fiber Optic Light Cable,
with straight connector, diameter 3.5 mm,
length 180 cm

495 NA

Same, length 230 cm

Cold Light Fountain XENON 300 SCB



20133101-1

Cold Light Fountain XENON 300 SCB
with built-in antifog air-pump, and integrated
KARL STORZ Communication Bus System SCB
power supply:
100–125 VAC/220–240 VAC, 50/60 Hz
including:

Mains Cord

SCB Connecting Cable, length 100 cm

20133027

Spare Lamp Module XENON
with heat sink, 300 watt, 15 volt

20133028

XENON Spare Lamp, only,
300 watt, 15 volt

Cold Light Fountain XENON NOVA® 300



20134001

Cold Light Fountain XENON NOVA® 300,
power supply:
100–125 VCA/220–240 VAC, 50/60 Hz
including:

Mains Cord

20132028

XENON Spare Lamp, only,
300 watt, 15 volt

Data Management and Documentation

KARL STORZ AIDA® – Exceptional documentation



The name AIDA stands for the comprehensive implementation of all documentation requirements arising in surgical procedures: A tailored solution that flexibly adapts to the needs of every specialty and thereby allows for the greatest degree of customization.

This customization is achieved in accordance with existing clinical standards to guarantee a reliable and safe solution. Proven functionalities merge with the latest trends and developments in medicine to create a fully new documentation experience – AIDA.

AIDA seamlessly integrates into existing infrastructures and exchanges data with other systems using common standard interfaces.



WD 200-XX* **AIDA Documentation System**,
for recording still images and videos,
dual channel up to FULL HD, 2D/3D,
power supply 100-240 VAC, 50/60 Hz
including:

USB Silicone Keyboard, with touchpad

ACC Connecting Cable

DVI Connecting Cable, length 200 cm

HDMI-DVI Cable, length 200 cm

Mains Cord, length 300 cm



WD 250-XX* **AIDA Documentation System**,
for recording still images and videos,
dual channel up to FULL HD, 2D/3D,
including SMARTSCREEN® (touch screen),
power supply 100-240 VAC, 50/60 Hz

including:

USB Silicone Keyboard, with touchpad

ACC Connecting Cable

DVI Connecting Cable, length 200 cm

HDMI-DVI Cable, length 200 cm

Mains Cord, length 300 cm

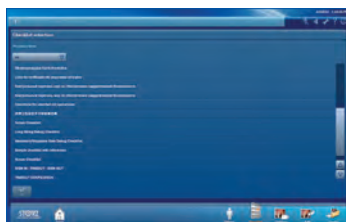
*XX Please indicate the relevant country code
(DE, EN, ES, FR, IT, PT, RU) when placing your order.

Workflow-oriented use



Patient

Entering patient data has never been this easy. AIDA seamlessly integrates into the existing infrastructure such as HIS and PACS. Data can be entered manually or via a DICOM worklist. All important patient information is just a click away.



Checklist

Central administration and documentation of time-out. The checklist simplifies the documentation of all critical steps in accordance with clinical standards. All checklists can be adapted to individual needs for sustainably increasing patient safety.



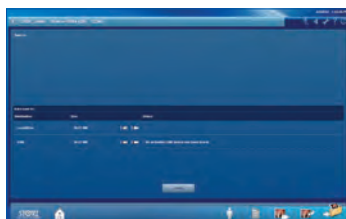
Record

High-quality documentation, with still images and videos being recorded in FULL HD and 3D. The Dual Capture function allows for the parallel (synchronous or independent) recording of two sources. All recorded media can be marked for further processing with just one click.



Edit

With the Edit module, simple adjustments to recorded still images and videos can be very rapidly completed. Recordings can be quickly optimized and then directly placed in the report. In addition, freeze frames can be cut out of videos and edited and saved. Existing markings from the Record module can be used for quick selection.



Complete

Completing a procedure has never been easier. AIDA offers a large selection of storage locations. The data exported to each storage location can be defined. The Intelligent Export Manager (IEM) then carries out the export in the background. To prevent data loss, the system keeps the data until they have been successfully exported.



Reference

All important patient information is always available and easy to access. Completed procedures including all information, still images, videos, and the checklist report can be easily retrieved from the Reference module.

Equipment Cart



UG 220

UG 220

Equipment Cart

wide, high, rides on 4 antistatic dual wheels equipped with locking brakes 3 shelves, mains switch on top cover, central beam with integrated electrical subdistributors with 12 sockets, holder for power supplies, potential earth connectors and cable winding on the outside,

Dimensions:

Equipment cart: 830 x 1474 x 730 mm (w x h x d),

shelf: 630 x 510 mm (w x d),

caster diameter: 150 mm

including:

Base module equipment cart, wide

Cover equipment, equipment cart wide

Beam package equipment, equipment cart high

3x **Shelf**, wide

Drawer unit with lock, wide

2x **Equipment rail**, long

Camera holder



UG 540

UG 540

Monitor Swivel Arm,

height and side adjustable, can be turned to the left or the right side, swivel range 180°, overhang 780 mm, overhang from centre 1170 mm, load capacity max. 15 kg, with monitor fixation VESA 5/100, for usage with equipment carts UG xxx

Recommended Accessories for Equipment Cart



UG 310

UG 310 **Isolation Transformer,**
200 V–240 V; 2000 VA with 3 special mains socket,
expulsion fuses, 3 grounding plugs,
dimensions: 330 x 90 x 495 mm (w x h x d),
for usage with equipment carts UG xxx



UG 410

UG 410 **Earth Leakage Monitor,**
200 V–240 V, for mounting at equipment cart,
control panel dimensions: 44 x 80 x 29 mm (w x h x d),
for usage with isolation transformer UG 310



UG 510

UG 510 **Monitor Holding Arm,**
height adjustable, inclinable,
mountable on left or right,
turning radius approx. 320°, overhang 530 mm,
load capacity max. 15 kg,
monitor fixation VESA 75/100,
for usage with equipment carts UG xxx

Notes:

